Elsevier Editorial System(tm) for Icarus
Manuscript Draft

Manuscript Number: ICARUS-13018R1

Title: The Microwave Properties of the Jovian Clouds: A New Model for the Complex Dielectric Constant of Aqueous Ammonia

Article Type: Regular Article

Keywords: Jupiter, Atmosphere; Jupiter, Clouds; Radio Observations; Atmospheres, Composition; Spectroscopy.

Corresponding Author: Dr. Paul Steffes,

Corresponding Author's Institution: Georgia Institute of Technology

First Author: Danny Duong, M.S. ECE

Order of Authors: Danny Duong, M.S. ECE; Paul Steffes; Sahand Noorizadeh, BSEE

Abstract: A new model for the complex dielectric constant of aqueous ammonia (NH4OH) under conditions characteristic of the Jovian clouds has been developed. The new model is based on laboratory measurements in the frequency range between 2 and 8.5 GHz for ammonia concentrations of 0-8.5 % by volume and temperatures between 274 and 297 K. The new model is based on the Meissner and Wentz (2004) model of the complex dielectric constant of pure water but contains corrections for dissolved ammonia. Assuming Raleigh scattering, these measurements are applied to a cloud attenuation model to calculate the range of opacity of the Jovian aqueous ammonia clouds. These measurements will improve our understanding of the data collected by the Juno microwave radiometer (MWR) by better characterizing the absorption properties of the aqueous ammonia present in the Jovian atmosphere.

The new model has been validated for temperatures up to 313 K, and may be consistently used for the expected conditions for aqueous clouds in all of the outer planets. The model fits 60.26 % of all laboratory measurements within 2-sigma uncertainty. A description of the experimental setups, uncertainties associated with the laboratory measurements, the model fitting process, the new model, and its application to approximating Jovian cloud opacity for NASA's Juno mission to Jupiter are provided.

RESPONSES TO REVIEWER COMMENTS, MS#13018 DUONG ET AL.

Our responses to Reviewer Comments are shown in boldface below each reviewer comment (shown in italics):

Reviewer #1: Review of Icarus ms# 13018: Duong, Steffes, and Noorizadeh - The microwave properties of the jovian clouds: A new model for the complex dielectric constant of aqueous ammonia.

This manuscript reports new laboratory measurements and a model fit to the complex dielectric constant of aqueous ammonia for temperatures and concentrations likely appropriate to the microwave remote sensing of Jupiter's troposphere. This work supports the upcoming radiometry investigation on the Juno Jupiter orbiter mission and could be of importance to the retrieval of vertical profiles of kinetic temperature, ammonia and water.

This reviewer unfortunately has no hands-on experience with the kind of laboratory work described in the report and would not know an Agilent 85070E dielectric probe if it fell into his lunch. I am, however, familiar with the published work of the second and corresponding author over many years and know him to be a highly skilled experimenter of great integrity. I am satisfied that Paul Steffes would not do anything wrong in the way of experimental procedure. (Although I am not familiar with the first and third authors, I assume their affiliation with the corresponding author in this effort certifies their competence.) I also have some familiarity with the atmospheric problems this work addresses and while I expect its publication to represent an important contribution to the literature, I feel that the submitted manuscript could benefit from some revision of its presentation. While some material could be removed or abbreviated, some parts of the discussion deserve further clarification and more interpretative context. Some figure captions appear to be just plain sloppily wrong. My specific suggestions and questions are listed below.

We thank the reviewer for his/her kind comment and appreciate the suggestions for improving the paper. The 1st and 3rd authors are recently graduated Georgia Tech students, so a "double" affiliation has been inserted into the new manuscript. We especially apologize for the figure captions being displaced. (This occurred when we loaded the .doc version of the paper into the Elsevier website and captions were pushed downward in the conversion to PDF, making them appear above the succeeding figures.) Of course, these have been corrected.

The last sentence of Section 1 (line 58 on p.5) refers to a "Figure 13." But there is no Figure 13 in my copy of the manuscript. Did the authors mean Figure 11?

The reviewer is correct; it should be "Figure 11." The typo has been corrected.

Eqns. (1) - (4) on pp. 7 and 8 give relationships between impedances, and other electromagnetic quantities including the complex permeability, conductivity, and complex dielectric constant. While no doubt of interest to the experimenter who makes the measurements, I find no numbers or plots or even any descriptive interpretation for any of

these except the dielectric constant. So what is the point of including these relations in the discussion?

The description of the measurement approach (which begins on page 6) states that the probe system operates by measuring the complex reflection coefficient of the probe when immersed in the test liquid. However, it is the *complex dielectric constant* of the cloud liquid which is needed by those modeling the effects of clouds on the microwave spectrum of the outer planets. Since this measurement technique has not been previously presented in *ICARUS*, it was felt that the readers deserved a brief explanation of how the measured quantity was related to the presented results. We have changed the wording to make this more understandable.

The semi-sinusoidal variation of the measured imaginary part of the dieletric constant over frequency, as shown in Figure 2, apparently corresponds to the "systematic standing wave among all data sets due to reflections from the test setup," as mentioned in line 144 on p.10, but this might bear repeating in the caption. Although the given explanation sounds plausible, can the authors give further assurance that the indicated correction factor derived in terms of the measured departure from the Meissner and Wentz model is in fact applicable to the measurement of aqueous ammonia at different temperatures? Did they measure pure water at a different temperature and get the same correction function?

The reference to the "systematic standing wave" has been included in the caption for Figure 2. Pure water was measured at all temperatures used. The correction function was nearly identical at 40°C and 24°C, but because the 4°C system was enclosed in a compact refrigerator (Figure 4), the additional correction for reflections of the microwave signals "off the walls" of the refrigerator required a different correction function. This is now referenced in the paper.

On p.18, the reader learns that 26 data sets were taken, 11 at ~24°C and 15 at ~4°C. How can a measured correction at these two temperature settings be used to derive new results for temperatures up to 40°C? The last sentence before the acknowledgements on p.36 does finally state that "Limited additional measurements at higher temperatures show that the model can be reliably used to temperatures exceeding 40°C (313K)" but that seems a little late to explain a result stated in the abstract.

This comment is well taken. In the original draft, we were going to include a block diagram of the 40°C system and present the data taken, but because of the volatility of the ammonia solution at that temperature, only a very limited range of ammonia concentration could be maintained (0.71-0.82%), and for only very short periods of time. Because of the limited range of ammonia concentration in those mixtures, that data was not used in derivation of the model. However, that data served as a "check" of the model at higher temperature. This has been added to the manuscript.

In eqn. (5) on p.18, why do the authors bother to include the last term factored by the conductivity, since this is stated to be zero for the assumed absence of salinity (S=0)? Again, why does this equation, along with (6)-(10), include the indicated dependence on S,

since this is assumed to be zero? Perhaps the authors think that as a matter of scholarship it is important to explicitly expose the conformance of their expressions with those presented by Meissner and Wentz (2004)? I would guess that few readers and users of this work will actually consult that paper. (I have, however, checked the correct transcription from that paper of these equations and the numerical parameters given in Table 2.) My concern is that in the interest of avoiding typographical or transcription errors the key expressions be stated as simply and cleanly as possible.

This comment is also well taken. The equations have been restated without reference to salinity.

The discussed revision of the preliminary Eqn. (16) to the slightly modified Eqn. (17) seems clumsy. Is there some way of revising the derivation and discussion of these two on pp. 24 and 25 into some more concise treatment of a single correction equation?

Done!

In line 335 on p.25, "fit" should read "fits".

Corrected!

There seem to be many mistakes in the figure captions, as if those for part "a" were simply copied and pasted for part "b" without amendment. It looks as if caption 6b should be changed to read "at 0.85%" instead of "at zero ammonia concentration" and "22.1 and 3.0 degrees Celsius", instead of "22.5 and 3.6", consistent with the boxed-in legend. (And what is the figure without a caption on p.26?) Fig.7b should probably read "1.7 % NH3/volume" instead of "0.85%", consistent with its label at the top. Figure 8b should probably read "3.4%" instead of "1.7%" and "20.7 and 3.0" instead of "21.7 and 3.6". Figure 9b should probably read "8.5%" instead of "3.4%", and "3.0 degrees Celsius" is inconsistent with "3.2°C" in the boxed-in legend. And where is the figure to go with the caption for 10b?

As previously mentioned, we especially apologize for the figure captions being displaced. (This occurred when we loaded the .doc version of the paper into the Elsevier website and captions were pushed downward in the conversion to PDF, making them appear above the succeeding figures.) Of course, these have been corrected.

Eqn (19) on p. 32 finally exposes the key relation between the new measurements and the opacity contribution of the aqueous ammonia to the total absorption in the radiative transfer equation, as needed for the retrieval of kinetic temperature and chemical abundances. For me the paper would be better presented with this as the first numbered equation, but I will leave it to the authors to think about that. I am surprised to see the units for alpha given as "dB/km." Is this and the specification of wavelength in km some new standard? (I believe an author should be permitted his own choice of units, but would appreciate some indication of the reason for the choice and a warning for comparison with other published work.) I assume that the total absorption coefficient will include with this

the sum of separate contributions for ammonia inversion and rotation bands, along with hydrogen collision-induced dipole radiation bands, plus water vapor and liquid? Could the authors please provide an estimate of the likely or considered range of the relative proportion of the aqueous ammonia contribution to the others, say near a frequency where the effect is the largest? If the expected contribution is relatively small, then we can regard this as a minor correction to the retrieval of temperature, ammonia, and water. But if it is large, then we are looking at the need to add the aqueous ammonia concentration C to our list of things to be accurately retrieved or if necessary plausibly assumed as an added caveat to the deep sounding of Jupiter. This is an important issue and the authors are now in a better position to address it than anyone else.

While we appreciate the reviewer's comments, we have decided to keep Eqn. 19 toward the end of the paper, since it represents the application of the measured quantities, which logically belongs in the concluding sections of the paper. This equation is well known to nearly all involved in radio scientific studies of terrestrial or planetary atmospheres, so it is not a "surprise" to most readers. Regarding the use of dB/km, those units are most commonly used in engineering, but are uniquely defined so as to avoid any ambiguity between field extinction coefficients and radiation intensity extinction coefficients. We have used these units in over 40 refereed journal papers including Icarus, JGR-Planets, Space Science Reviews, and Radio Science. In the revised paper, we have included a description of how these units relate to others commonly used (as we did in previous papers).

The use of km for the wavelength is related to the units desired for the extinction (absorption) coefficient. Given the relatively low opacity of the clouds, the use of km is preferred.

To fully discuss the proportion of the microwave opacity from the clouds relative to other gaseous constituents such as ammonia, water vapor, hydrogen sulfide, phosphine, and collisionally-induced absorption from hydrogen, a much more extensive (or additional) paper would be necessary wherein the description of all of the models used to make such a comparison is given, in addition to assumptions made regarding the potential ranges of constituent abundances, cloud bulk density, and sedimentation schemes. For Jupiter, such extensive discussions are included in the Karpowicz (2010) dissertation and to a smaller extent in the 2005 paper by Janssen et al. A new paper by Janssen et al. (2013, MWR: MICROWAVE RADIOMETER FOR THE JUNO MISSION TO JUPITER) has been submitted for a special Juno issue of Space Science Reviews and will contain a more complete discussion. For Saturn, the recent paper by Janssen et al. (Sept-Oct 2013, Icarus v.226 pp. 522-535) gives a clear description of the comparative opacities. We have added all of these references to the revised paper.

At the top of Fig.12, "Jovian Ammonia Clous" should read "Clouds". It seems to me that this plot does not make very good use of the space and colored ink, but may suggest that the relevant absorption is only very weakly sensitive to the concentration of aqueous ammonia. How about adding additional curves in this plot for the modeled absorption at

different temperatures and with concentrations up to 8%? If the curves are really that simple then it seems likely they could be represented by some much simpler polynomial than the algebraic sausage implied by Eqns. (18) and (19) with their 16 numerical parameters. And if so, I would encourage the authors to construct a simpler numerical fit to their representation of the absorption coefficient. Does a two sigma fit to "60.26%" (!) of all laboratory measurements really require 16 parameters, each given to four or five significant figures? I can think of examples of modern specifications of planetary parameters numerically fitted to ridiculous precision being mistakenly reported in the literature with typographical errors. Of course these things can be fixed after the fact in distributed computer kernals, but some people rely on the published sources.

The typo at the top of Figure 12 has been corrected. We agree with the reviewer that there is little advantage in presenting multiple plots of the absorption from a putative cloud with such a small variation in ammonia concentration. The objective of this plot is to give an example of a "typical" cloud absorption spectrum. Since the best models to date estimate a concentration of 2-3%, we use the 2.5% as the concentration in the new figure. Note that the sensitivity of cloud microwave opacity to ammonia concentration is well demonstrated in Figure 11.

The biggest uncertainty in estimating potential cloud opacity lies with bulk density. Different modelers have varied the estimated bulk density over a range from 0.1 to 100 g/m^3. Since the microwave opacity is linearly proportional to bulk density, we have chosen to use 1 g/m^3 as the representative bulk density. The reader can scale it by their preferred value.

Again in the interest of simplicity, I am concerned about the adopted Celsius temperature scale for the model fit. While this may be a common standard for both oceanography and lab measurements, the Juno microwave science will be using the Kelvin scale, as does Figure 12 of the manuscript. Would the authors consider the construction of some simpler numerical fit, as facilitated by modern mathematical software packages, giving the result in terms of the Kelvin temperature scale?

While a numerical fit related to the Kelvin temperature scale of our limited data would be more convenient, it would sacrifice the years of work done by our terrestrial atmospheres and ocean science colleagues to most accurately represent the microwave properties of pure water. Additionally, because of the change-of-state of water at 0°C, many modelers have found that more direct expressions could be derived using the °C scale. Our new model has now been implemented at 5 universities and at JPL, and we've received no complaints from programmers or scientists regarding the ease of implementation into their radiative transfer models, all of which use temperature profiles in Kelvins.

Again, I consider this to be a good and important piece of work and I am confident that the authors know what they are doing. But I recommend some revision for the sake of clarity and ease of accurate application, as well as the interpretative context of the atmospheric science, along the lines outlined here.

Once again, we sincerely thank the reviewer for his/her suggestions for improving the paper. We have implemented nearly all suggested changes, and deeply appreciate the resulting improvement.

Reviewer #2: Reviewers Comments

Manuscript Number: : ICARUS-13018
Title: The Microwave Properties of the Jovian Clouds: A New Model for the Complex Dielectric Constant
Authors: Danny Duong, Paul G. Steffes, Sahand Noorizadeh

General Comments:

This manuscript discusses a new model for the complex dielectric constant of aqueous ammonia (NH4OH) under conditions characteristic of the Jovian water clouds. The new model is based on laboratory measurements in the frequency range between 2 and 8.5 GHz, and for ammonia concentrations of 0-8.5 % by volume and temperatures between 274 and 297 K. The authors emphasizes that this new model is important to the understanding of the data collected by the Juno microwave radiometer (MWR) at Jupiter. The authors also mention that their model may be used consistently for aqueous clouds in all the outer planets.

The model presented in this paper is based on is based on the Meissner and Wentz (2004) model of the complex dielectric constant of pure water, but with corrections for dissolved ammonia. These corrections were obtained using a dielectric probe measurement system (Agilent 85070E), presumably set up at the Georgia Institute of Technology.

This is important work and it is appropriate that the paper be published in Icarus. Many Icarus readers will be interested in this paper. A number of specific comments about the paper follow. I recommend publishing the paper after the authors have responded to the Specific Comments below.

We thank the reviewer for his/her kind comments and appreciate the suggestions for improving the paper.

General Comments

It would help if you provided units for the parameters you used. For parameters that are dimensionless, give the value of the normalization constant and dimensions.

Since the dielectric constants are unitless, all of the parameters are unitless. The normalization constants for some of the constants from the original Meissner and Wentz model are normalized to multiple powers of inverse temperature, making statement of the normalization constant difficult, which is likely why those authors

didn't provide those values. The coefficients for our correction term are either exponents or coefficients normalized by multiple powers of inverse temperature, frequency and volume concentration, making the unit definition cumbersome and of little use to the reader. (They could obviously be directly determined from the expressions.)

All of the Figures use printing that is hard to read. I suggest you improve the quality of the figures.

The printing on the figures has been adjusted to improve readability.

The ordinate axes are unlabeled in many of the figures.

All ordinates are now labeled.

My preference would be to label the frequency scales in all of the figures in GHz rather than having the reader figure out what you mean by the hanging x109 at the end of ordinate scale. Note also that you use frequency in GHz in the equations for permittivity.

Agreed, all abscissas are now in units of GHz.

You use the symbol <sigma> for both conductivity and uncertainty.

This has now been corrected. The symbol σ is only used for uncertainties (i.e., where sigma is the widely known term for standard deviation).

Specific Comments:

L58,P5 (Line 58-Page 5) - My copy of the manuscript contains 12 Figures. This line mentions an important Figure 13, not present in my copy.

The reviewer is correct; it should be "Figure 11." The typo has been corrected.

L86,P6 - Give the algorithm that was used to convert the pH to ammonia concentration. Define the concentration - is it molar concentration? How is volume defined?

An ammonia concentration verification procedure was performed to develop an empirical relationship between ammonia concentration and pH, as measured in the testing environment in our laboratory. As discussed on pages 16 and 17 of the manuscript, two trials for each concentration (i.e., 0.85, 1.7, 3.4, and 8.5 nominal percent NH3/volume as provided by the supplier) were performed with 30 measurements for each trial. This provided a linear piecewise correlation between the ammonia concentration and pH. This is now more clearly described.

As shown in Table 1, over a time period of 20 minutes, ammonia concentration did not grossly preferentially evaporate from aqueous ammonia solutions exposed to air.

Equation 2 - In the equation for the load impedance, ?, is defined as the electric permittivity. Is this the same ? as used in L101? Is it real or imanginary when used in Eq 2? With <sigma> = 0, it might be clearer to write Eq 3 as

ZL = ?(mu/?)

The reviewer is correct. We have restructured the introductory equations to make more clear the relationship between the measured complex reflection coefficient and the presented values for the complex dielectric constant.

L144, P10 - The correction factor for the imaginary part of the dielectric constant shown in Figure 2 is small in the 2-4 GHz range but is almost a factor of 2 near 7.5 GHz. You mention a systematic standing wave as being responsible for this large correction. Can you explain the origin of the standing wave in more detail and why you believe the same correction factor you use for pure water also applies when you add NH3 to pure water.

By inspecting Figure 2, the readers views the standing wave on the transmission line between the network analyzer and the probe (which appears as a standing wave in frequency with wavelength ~3 GHz), which is generated by the poor match between the transmission line (impedance 50 ohms) and the material under test (scalar impedance less than 1 ohm). The resulting additional changes in impedance caused by the introduction of ammonia into the solutions has minimal effect on the magnitude of the correction factor. Moreover, the frequency dependence of the correction factor is only a function of the cable length, which does not change during our experiments.

Can you show a companion figure to Figure 2 which shows how well your instrumentation measures the real part of the dielectric constant.

We initially did not include a companion figure showing the correction to the real part of the dielectric constant since it "told the same story" as the correction of the imaginary part. (Percentage wise, it was less than the corrections to the imaginary part, so we picked the most severe case.) We do have a plot available of the raw data for the real part complex dielectric constant of pure water versus the reference model of Meissner and Wentz (Figure 15 in Duong's thesis (2011). However, it doesn't have the third curve showing the correction factor. Since we feel this would only further confuse the readers, we ask to keep Figure 2 as it currently stands.

Figure 3 - Explain why the water lab data does not coincide exactly with the Meissner/Wentz model after you apply the correction factor. I thought the correction factor was the difference between the lab data and the Meissner/Wentz model.

The correction factor was obtained by a linear difference between the Meissner and Wentz model and the average of three calibration measurements of pure water at each temperature (23±0.5 degrees Celsius for room temperature and 4.5±1.7 degrees Celsius for cold temperature). Figure 3 presents the correction factor applied to a single one of these pure water calibration measurements.

L320,P24 - Do the real and imaginary components yield minimum functions simultaneously?

No, the best fits for real and imaginary components were derived completely independently. This is now made clear in the text.

Equation 18 - Since <epsilon> ? depends on S in the Meissner/Wentz formulation, what is the justification for treating this term without a dependence on C.

Of course, since S is the salinity of the water, it would be zero in a Jovian cloud. However, the reviewer is correct in that as an electrolyte, the presence of dissolved ammonia could have similar effects on the dielectric properties of water. The sources of microwave opacity lie both in the induced conductivity and in the modification to the relaxation time of pure water. Since only a limited number of conductivity measurements have been conducted with aqueous ammonia (and only up to a frequency of 25 kHz), it would have been very speculative (and not really necessary for this work) to try to split the two effects as did Meissner and Wentz for salt water. It is noteworthy that our correction terms are of a form similar to the component due to relaxation time

Figure 6a and 6b - How about putting the Meissner/Wentz data on these two plots for which C = 0.

There are 8 data points referenced in Meissner and Wentz in the 2-8 GHz frequency range. They were all taken at a temperature of 25°C, which is slightly higher than our room-temperature data (22.5°C). We have added those datapoints as requested. Note that this REQUIRES using color for Figures 6a and 6b. Adding these points makes the figures very "busy," but we are willing to meet the reviewer's request.

Figure 8b and 9b show redundant values of the real component of the dielectric component near 3.5 GHz for two different temperatures. Does the Meissner/Wentz data show a similar redundancy.

There is a long list of experimenters who have measured this redundancy. It is related to the shift of the Debye relaxation times of the liquid water with temperature which (at certain "magic" frequencies") results in a real component of the dielectric constant which is nearly independent of temperature.

L390, P31 - Why do you conclude that the deviations discussed here are caused by

resonances in the enclosed refrigerator. Is there an explanation of why the resonances show up at cold temperatures?

The temperature chamber (refrigerator) used for the lower-temperature experiments has metallic walls and is of such dimensions that it has several microwave resonances which can be stimulated by our probe. While it would have been advantageous to purchase and line the interior of the chamber with microwave absorbing material, it was not considered to be necessary to achieve the precisions we required.

The Microwave Properties of the Jovian Clouds: A New Model for the Complex Dielectric Constant of Aqueous Ammonia

Danny Duong[1,2]
dduong16@gmail.com

Paul G. Steffes[1]
Telephone: 404-894-3128
Fax: 404-894-5935
steffes@gatech.edu

Sahand Noorizadeh[1,3]
sahand.noorizadeh@gmail.com

[1] School of Electrical and Computer Engineering, Georgia Institute of Technology, Atlanta, GA 30332-0250
[2] MPR Associates Inc., Alexandria, VA 22314
[3]Tektronix Inc., Beaverton, OR 97077

Submitted: 30 June 2013
Revised: 31 October 2013

43 pages; 6 tables, 17 figures.

Proposed Running Head: Microwave Opacity of Jovian Clouds
Please send all editorial correspondence to:

Paul G. Steffes
School of Electrical and Computer Engineering
Georgia Institute of Technology
Atlanta, GA 30332-0250

Phone: 404-894-3128
Fax: 404-894-4641
Email: **steffes@gatech.edu**

Abstract

A new model for the complex dielectric constant of aqueous ammonia (NH_4OH) under conditions characteristic of the Jovian clouds has been developed. The new model is based on laboratory measurements in the frequency range between 2 and 8.5 GHz for ammonia concentrations of 0-8.5 % by volume and temperatures between 274 and 297 K. The new model is based on the Meissner and Wentz (2004) model of the complex dielectric constant of pure water but contains corrections for dissolved ammonia. Assuming Raleigh scattering, these measurements are applied to a cloud attenuation model to calculate the range of opacity of the Jovian aqueous ammonia clouds. These measurements will improve our understanding of the data collected by the Juno microwave radiometer (MWR) by better characterizing the absorption properties of the aqueous ammonia present in the Jovian atmosphere.

The new model has been validated for temperatures up to 313 K, and may be consistently used for the expected conditions for aqueous clouds in all of the outer planets. The model fits 60.26 % of all laboratory measurements within 2-sigma uncertainty. Descriptions of the experimental setups, uncertainties associated with the laboratory measurements, the model fitting process, the new model, and its application to approximating Jovian cloud opacity are provided.

Key Words: Jupiter, Atmosphere; Jupiter, Clouds; Radio Observations; Atmospheres, Composition; Spectroscopy.

1. INTRODUCTION

It is well understood that the microwave emission spectrum of Jupiter's troposphere reflects the abundance and distribution of constituents such as ammonia, water vapor, and potentially from aqueous ammonia clouds (see, e.g., Janssen et al., 2005), but there are a number of factors that limit the accuracy of this approach for microwave remote sensing of these constituents (de Pater et al., 2005). The most critical of these is the knowledge of the microwave absorption properties of these constituents under Jovian conditions. While effects of upper-level crystalline clouds have negligible effect on the centimeter-wavelength emission from Jupiter, putative tropospheric clouds of liquid aqueous ammonia (liquid water with dissolved ammonia) may have detectable influence on its centimeter-wave emission signature (see, e.g., Janssen et al., 2005). To date, nearly all microwave radiative transfer models incorporating effects of aqueous clouds employ the measured properties of pure water to estimate the effects of such clouds. However, the effect of dissolved constituents on the dielectric properties of condensed water can be significant, and no laboratory measurements of the effect of dissolved ammonia on the microwave properties of such condensates have been conducted. Depending on the local abundance of water vapor, liquid aqueous clouds with dissolved ammonia likely form near the 6-10 Bar level of the Jovian atmosphere. (See e.g. Atreya *et al*. 1999.) While the actual bulk densities of such clouds are not known, the maximum possible values (corresponding to the amounts of each condensate exceeding the saturation vapor pressure at each altitude) are significant in that they could be dense enough to affect the atmospheric microwave emission spectrum (see, e.g., Janssen *et al.* 2005 or de Pater *et al.* 2005). In previous radiative transfer models of the microwave

emission from Jovian atmospheres, the complex dielectric constant of the cloud liquid was assumed to be approximately that of water (see, e.g., Janssen *et al.* 2005 or de Pater *et al.* 2005) since the dissolved ammonia concentration is expected to be relatively low (approximately 2-3%, by volume) due to the relatively low abundance of ammonia (see, e.g. Atreya et al., 1999). This assumption was made since no model existed for the complex dielectric constant for aqueous ammonia.

In this work, a model for the complex dielectric constant of aqueous ammonia (NH_4OH) has been developed based on several thousand new laboratory measurements in the frequency range between 2 and 8.5 GHz and at temperatures from 274-297 K using a dielectric probe measurement system. This new model is a significant step in better understanding the microwave properties of aqueous ammonia and is useful for characterizing cloud opacity of aqueous ammonia clouds under Jovian conditions. Presented in Figure 11 are the results from the new model showing how dissolved ammonia in the range between 0.85% to 8.5% (by volume) enhances the microwave opacity of an aqueous cloud.

2. MEASUREMENT THEORY AND SYSTEM

As shown in Figures 1, 4, and 5, the measurement systems developed for this work employ an Agilent 85070E dielectric probe, operating in conjunction with an Agilent E5071C network analyzer. The probe acts as an open-ended transmission line. The provided Agilent software directs the network analyzer to generate and transmit a signal over a specified microwave frequency range to the test material (water and aqueous ammonia for this work) via the probe, to then measure the reflected response, and finally to relate the reflected signal to the material's dielectric properties.

The Agilent 85070E dielectric probe has a relatively poor absolute accuracy of ±5% for the real part of the complex dielectric constant, E_r' (Agilent Technologies, 2006). To mitigate the uncertainty due to the dielectric probe instrumentation error, initial measurements of the complex dielectric constant of deionized water (DI water) were made. The complex dielectric properties of water have been previously measured to high accuracy by Meissner and Wentz (2004), and those measurements were used to provide a baseline correction of data taken with the Agilent 85070E dielectric probe. Measurements of the complex dielectric constant of test solutions were made in the 2– 8.5 GHz range. A complete sequence or data set recorded 30 sweeps/measurements with 1000 linearly spaced data points in the specified frequency range. Multiple measurement sequences were taken of each solution per temperature to develop a statistic for the variability in the data sets. The measurements recorded are tabulated in Table 5.

The complex dielectric constant of water varies with temperature, and it was assumed that the dielectric properties of aqueous ammonia would likely have a similar temperature dependence. Temperature was carefully monitored for each set of measurements so as to verify this assumption. Due to the volatile nature of aqueous ammonia and the high vapor pressure of NH_3 relative to water, preferential evaporation of NH_3 from the aqueous ammonia solutions was expected. Thus, the pH of the solution under test was recorded for each set of measurements so as to verify the ammonia concentration.

The probe software calculates the dielectric properties of the test material by measuring the complex reflection coefficient, Γ, at the boundary between the probe and the material under test, and relating this parameter to the material's

complex dielectric constant. In transmission line theory, the complex reflection coefficient (or the ratio of the reflected signal to the incident signal) is given by

$$\Gamma = \frac{V^-}{V^+} = \frac{Z_L - Z_0}{Z_L + Z_0} \quad (1)$$

where V^+ is the incident transmitted signal voltage, V^- is the reflected signal voltage, Z_L is the impedance of the load or material under test (MUT), and Z_0 is the characteristic impedance of the transmission line in ohms (Hayt and Buck 2006). For a dielectric material, the complex load impedance can be expressed as

$$Z_L = \sqrt{\frac{\mu}{\varepsilon}} \quad (2)$$

where μ is the magnetic permeability and ε is the complex dielectric permittivity of the medium which is defined as $\varepsilon = \varepsilon' - j \cdot \varepsilon''$. The concept of a complex electric permittivity arises from the non-ideal nature of materials relating to permanent or induced dipole relaxation, resonance effects of atoms, ions, or electrons, and conduction effects of dielectric materials (Hayt and Buck 2006). Thus, in a non-magnetic material, the load impedance can be expressed as

$$Z_L = \sqrt{\frac{\mu o}{(\varepsilon' - j \cdot \varepsilon'')\varepsilon_o}} \quad (3)$$

where μ_o is the magnetic permeability of free space, ε_o is the permittivity of free space, and where ε' and ε'' are the real and imaginary parts, respectively, of the complex dielectric constant of the load or MUT.

The resulting relationship between the complex dielectric constant and the complex reflection coefficient measured by the network analyzer is given by

$$\varepsilon = \varepsilon' - j \cdot \varepsilon'' = (377/Z_0)^2 (1 - \Gamma)^2 / (1 + \Gamma)^2 \quad (4)$$

where 377 ohms = $(\mu_o/ \varepsilon_o)^{0.5}$ is the characteristic impedance of free space and Z_o is the characteristic impedance of the transmission line (in our case, 50 ohms).

2.1 Room Temperature Measurement System

The measurement system used for room temperature measurements for this work is shown in Figure 1. The main component of the system is the Agilent 85070E dielectric probe. The dielectric probe is connected to an Agilent E5071B/C vector network analyzer (VNA) which is controlled by the Agilent 85070E software. Custom software in MATLAB® was developed to automate the data acquisition.

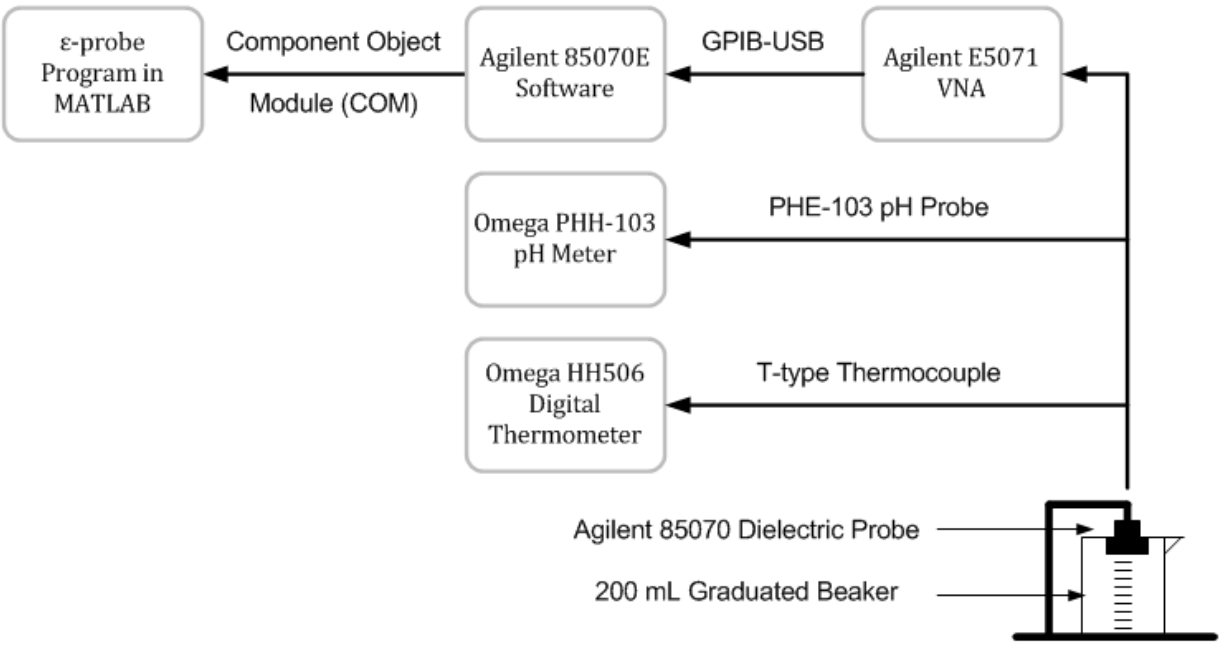

118

119 **Figure 1.** Block diagram of the room temperature measurement system.

120 Solutions were tested in a 200 mL graduated beaker. The temperature and pH of the
121 solution were monitored using the HH506 digital thermometer and Omega PHH-103
122 pH meter, respectively, to verify the temperature and concentration of ammonia. The
123 Omega PHH-103 has a pH measurement resolution of 0.01 and an accuracy of ±0.02.
124 The Omega HH506 digital thermometer has a temperature resolution of 0.1 ^{o}C and an
125 accuracy of ±(0.05 % rdg (^{o}C) + 0.3 °C) when using a T-type thermocouple.

126 The Agilent 85070E dielectric probe has a calibration process that was used before each
127 set of sequence of measurements at a particular temperature, i.e., one calibration for all
128 measurements at a given temperature. The absolute accuracy of these lab measurements
129 depends on the accuracy of measurements of the properties of aqueous ammonia
130 solutions relative to the reference (water). Water was chosen as the reference
131 measurement because its properties are well documented (Meissner and Wentz 2004). By

performing relative measurements with a well-known reference versus absolute measurements, the errors associated with the measurement system are decreased.

The water calibration is performed by taking three measurement sequences of pure water at each temperature (23 ± 0.5 °C for room temperature and 4.5 ± 1.7 °C for cold temperature), and correcting their average to fit the Meissner and Wentz model for pure water. The correction factor is obtained from the water measurements using a linear difference operation on the data so that it conforms to the Meissner and Wentz model. The linear correction was chosen over other possible mathematical operators because it was able to correct for systematic fluctuations easily. For example, the measurements of both the real and imaginary parts of the dielectric constants exhibited a residual standing wave of ~3 GHz length which could not be properly corrected for using a ratio-based correction factor.

A sample plot of a water data set at 23.9 °C (imaginary part of dielectric constant), the Meissner and Wentz model at 23.9 °C, and the correction factor applied to all room temperature measurements is shown below in Figure 2. There exists a systematic standing wave among all data sets due to reflections on the transmission line resulting from the impedance mismatch between the transmission line and the material under test. There also exists smaller higher frequency ripples in the overall spectral response, especially in the cold-temperature data, caused by microwave resonances in the metallic temperature chamber enclosure (refrigerator) stimulated by the probe. The same data set with the correction factor applied is shown in Figure 3.

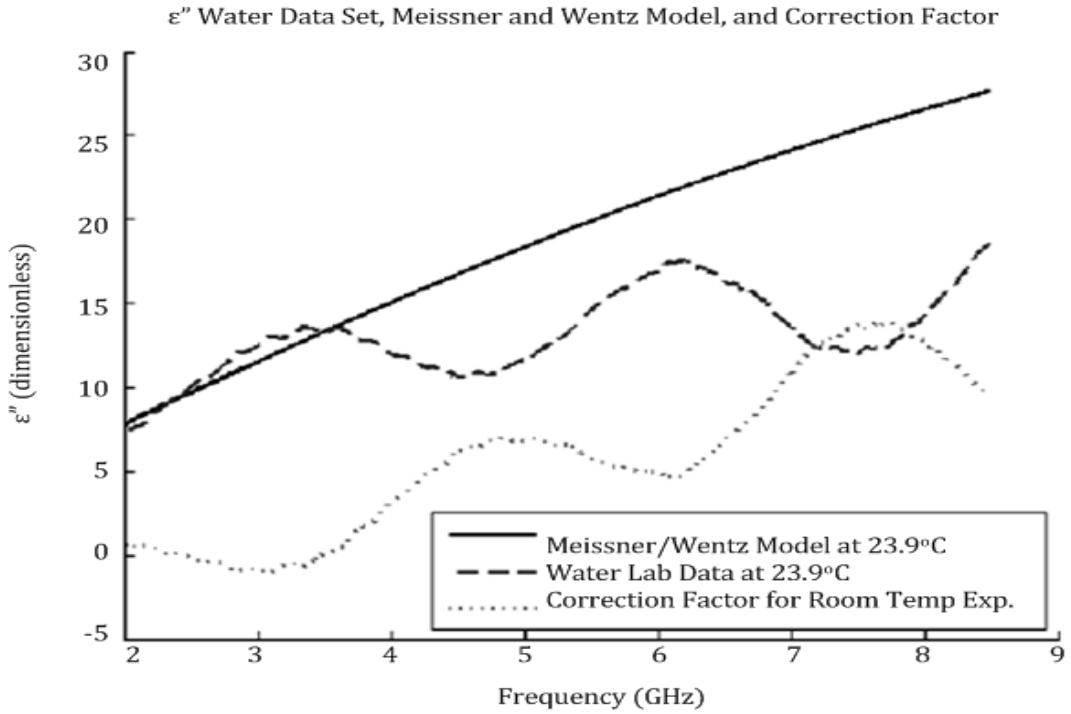

153

154 **Figure 2.** Meissner and Wentz model for imaginary part of dielectric constant and correction
155 factor for all room temperature measurements. The laboratory data shows a standing wave
156 feature resulting from the mismatch between the impedance of the transmission line with that of
157 the material under test. The correction factor is a linear difference operation of all water
158 measurements at room temperature and the model.

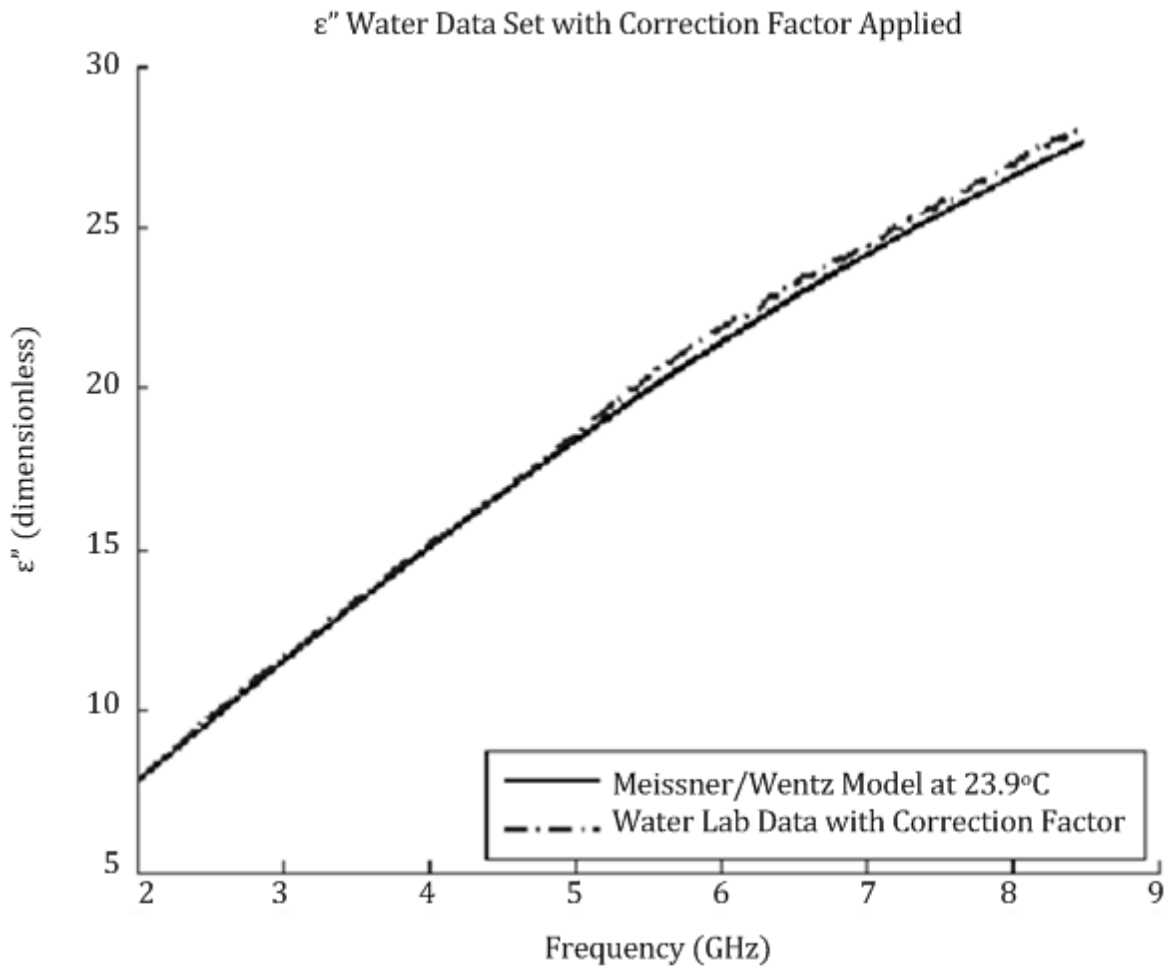

159

160 **Figure 3.** One of the three water data sets taken at 23.9 °C adjusted using the room
161 temperature correction factor, compared with the Meissner and Wentz (2004) model.

162 **2.2 Cold Temperature Measurement System**

163 Due to the volatility of aqueous ammonia, especially at higher temperatures, it
164 was determined that cold temperature measurements would provide a more reliable
165 data set to develop a model for the temperature dependence of the complex dielectric

properties of aqueous ammonia. A block diagram of the cold temperature measurement is shown in Figure 4.

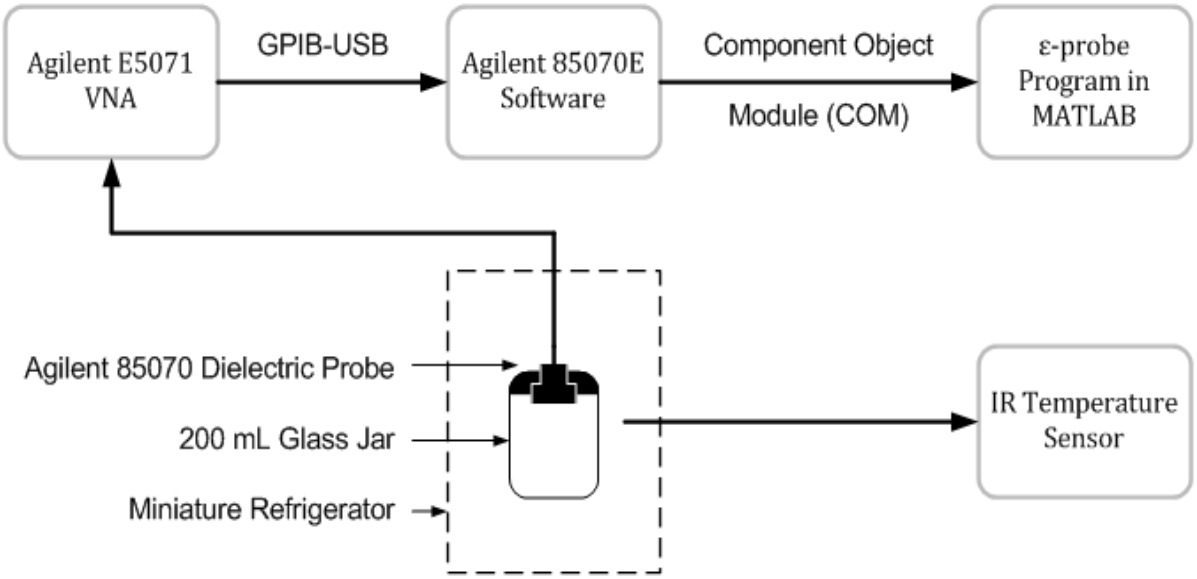

Figure 4. Block diagram of the cold temperature measurement system.

A miniature refrigerator was used to cool the solutions under test; the refrigerator was able to maintain a temperature of 4 °C ± 0.6 °C. Since aqueous ammonia is more stable at colder temperatures, continuous monitoring of the pH of the solutions under test was not necessary for the cold temperature measurements. Temperature was monitored with a Fluke 62 miniature IR thermometer which has a resolution of ±1 °C and an accuracy of ±1.5 °C. Temperature was monitored with the IR thermometer because it would not interfere with the dielectric probe measurement system and eliminated the need for an analog system. As with the room-temperature measurements, the water calibration is performed by taking three measurements of the

complex dielectric properties of pure water at 4.5 °C, and correcting them to fit the Meissner and Wentz model for pure water.

2.3 High Temperature Measurement System

To verify the effect of changes in temperature on the complex dielectric properties of aqueous ammonia, a high temperature measurement system was also designed. Initially, the high temperature system was identical to the room temperature system shown in Figure 1 with the dielectric probe and solution in test in an oven. An Omega CN77000 temperature controller was used with a T-type thermocouple to control the oven temperature. The Omega CN77000 has an accuracy of ±0.4 °C and could maintain the oven temperature to within ±2 °C of the set temperature value. The Omega HH506 digital thermometer, and later the Omega PHH-103 pH probe, was used to monitor the temperature of the solution in test.

After initial tests, it was determined that ammonia was preferentially evaporating from the aqueous ammonia solutions under test. This is due to the higher vapor pressure of ammonia than water, and this was confirmed with pH measurements. To reduce the evaporation of ammonia, 200 mL glass jars with a screw-on PTFE lined cap machined to fit the 85070E dielectric probe were used. In order to monitor the pH over the period of heating and measurement without disturbing the solution in test, a second 200 mL sealed glass jar was used as an analog system. With this analog system, the Omega PHH-103 was fitted to the analog jar and

monitored both pH and temperature with ±0.02 °C and ±0.3 °C accuracy, respectively. The high temperature system is shown in Figure 5.

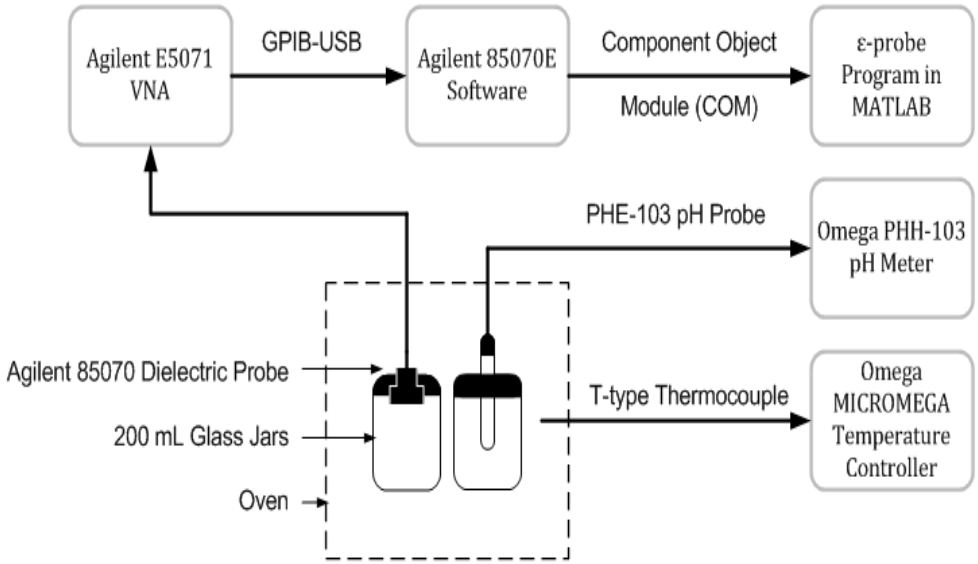

Figure 5. Block diagram of the high temperature measurement system. The dielectric probe is submerged in the sealed container on the left. The pH probe is submerged in an analog solution on the right. The T-type thermocouple which controls the oven temperature is shown on the right.

Measurements were conducted at 40 °C. However, because of the large amount of ammonia outgassing, only concentrations of 0.71-0.83 % were available for measurement. Accordingly, these measurements not used to develop the model but were used to verify the accuracy of the model developed from data taken at the two lower temperatures.

2.4 Verification of Ammonia Concentration

An accurate knowledge of the NH_3 concentration in the aqueous ammonia solutions under test is required for an accurate model of its properties. Access to a method to directly measure the ammonia concentration was not available for these measurements. However, a pH meter proved effective in monitoring the alkalinity of the aqueous ammonia solutions during test, and an independent pH study was performed to verify the validity of the pH measurements.

A sequence of 30 measurements of the complex dielectric properties of the aqueous ammonia solutions typically took 20 minutes to complete. For room temperature measurements, this was the only period in which the aqueous ammonia solution in test was exposed to the open air. Of major concern was the amount of NH_3 that evaporated from the aqueous ammonia solution during the experiment. The concentration verification experiments consisted of using a Vernier PH_BTA pH probe connected to a Vernier LabPro sensor interface to measure the pH of an identical solution of aqueous ammonia exposed to open air for a 20 minute period. The resolution of the Vernier PH_BTA probe is documented as 0.02 pH units, and the probe was calibrated using 4.0 and 7.0 pH buffer solutions before each trial. The probe was unable to measure the pH of deionized water due to the lack of any ionization, so only the pH of aqueous ammonia solutions were measured. The experiment consisted of placing the pH probe in a solution of aqueous ammonia at room temperature for five minutes to allow the meter to stabilize and then monitoring the pH for 20 minutes.

Two trials were performed for each concentration of aqueous ammonia; the results are shown in Table 1.

Table 1. Tabulated results for the concentration validation experiments.

Concentration (%NH_3/vol)	Trial	Minimum pH (pH units)	Maximum pH (pH units)	Mean pH (pH units)	Standard Deviation
0.85	1	11.48	11.53	11.500	0.0126
0.85	2	11.41	11.53	11.474	0.0309
1.7	1	11.66	11.73	11.698	0.0171
1.7	2	11.54	11.60	11.572	0.0198
3.4	1	11.72	11.89	11.795	0.0444
3.4	2	11.89	11.94	11.908	0.0136
8.5	1	12.04	12.23	12.124	0.0538
8.5	2	12.11	12.23	12.154	0.0284

As shown in Table 1 the standard deviation is low for the experiments, with only one 8.5 %NH_3/volume concentration trial having a standard deviation above 0.05 pH units. Particularly at the higher concentrations such as 3.4 % and 8.5 % NH_3/volume, there appears to be some loss in concentration over the span of 25 minutes. However, the change

in ammonia concentration is small relative to other uncertainties. These results made possible development of a linear piecewise correlation between ammonia concentration and the pH and allowed the development of reliable estimates of uncertainty in ammonia concentration during the experiements.

3. EXPERIMENTAL RESULTS AND MODEL FITTING

In total, 26 data sets were taken (11 at ~24 °C and 15 at ~4 °C). Using this data, a new model for the complex dielectric constant of aqueous ammonia has been developed which fits 60.26 % of all 780,000 measured data points within 2σ uncertainty. The model was developed as a corrective term to the model for the complex dielectric constant of pure water developed by Meissner and Wentz (2004). Meissner and Wentz's model is fit-based on laboratory measurements and is valid for temperatures between -20 °C and 40 °C and for frequencies up to 500 GHz for pure water. Their model is also valid for sea water for temperatures between -2 °C and 29 °C and for frequencies up to 90 GHz.

Meissner and Wentz (2004) implement a double Debye fit in their model of the complex dielectric constant of pure and sea water; their model for pure water is given below in equations 5-10. Temperatures are in °C, and frequency (ν) is in GHz.

$$\varepsilon(T,S) = \frac{\varepsilon_s(T) - \varepsilon_1(T)}{1 + j \cdot \frac{\nu}{\nu_1(T,S)}} + \frac{\varepsilon_1(T) - \varepsilon_\infty(T)}{1 + j \cdot \frac{\nu}{\nu_2(T,S)}} + \varepsilon_\infty(T) \quad (5)$$

$$\varepsilon_S(T) = \frac{3.70886 \cdot 10^4 - 8.2168 \cdot 10^1 \cdot T}{4.21854 \cdot 10^2 + T} \tag{6}$$

$$\varepsilon_1(T) = x_0 + x_1 \cdot T + x_2 \cdot T^2 \tag{7}$$

$$\nu_1(T) = \frac{45 + T}{x_3 + x_4 \cdot T + x_5 \cdot T^2} \tag{8}$$

$$\varepsilon_\infty(T) = x_6 + x_7 \cdot T \tag{9}$$

$$\nu_2(T) = \frac{45 + T}{x_8 + x_9 \cdot T + x_{10} \cdot T^2} \tag{10}$$

In equation 5, $j = \sqrt{-1}$ and ν_1 and ν_2 represent the two Debye relaxation frequencies in GHz. The parameters x_k are given below in Table 2.

Table 2. Parameters for the Meissner and Wentz model.

k	x_k
0	5.7230 E 00
1	2.2379 E -02
2	-7.1237 E -04
3	5.0478 E 00
4	-7.0315 E -02
5	6.0059 E -04
6	3.6143 E 00
7	2.8841 E -02
8	1.3652 E -01
9	1.4825 E -03
10	2.4166 E -04

3.1 Measurement Uncertainty

Two sources of uncertainty exist for the measurements: instrumentation errors and electrical noise (Err_{inst}) and conditional errors (Err_{cond}), which reflect the uncertainties in environmental conditions during the experiments. The term Err is used to describe a bound on uncertainty of 2σ, where σ is the standard deviation of the error process.

Instrumentation errors arise due to systematic offsets in the internal electronics of the test equipment used. Since these measurements are made relative to a well-measured reference fluid (pure water), the absolute uncertainty associated with measurements using the Agilent E5071C VNA is not significant. The electrical noise from the test equipment has a much larger effect, but is partially mitigated by taking 30 sweeps of measurements for each data set. The uncertainty that arises from electrical noise is modeled as a probability distribution of the 30 measurements per data set. The probability distribution chosen is the Student's t-test with a 95 % confidence interval (Hines *et al.* 2003), which is approximately equivalent to 2σ uncertainty (95.4%). For a data set of 30 measurements, Err_{inst} is calculated as

$$Err_{inst} = \frac{t_n}{\sqrt{n}} \cdot S_n \tag{11}$$

where n is the number of samples in the distribution (30), t_n is the Student t-test coefficient (critical value) for a 95% confidence interval, and S_n is the sample standard deviation. Common t-test values for 95% confidence are tabulated in Table 3, and the sample standard deviation is calculated as

$$S_n = \sqrt{\frac{1}{n-1}\sum_{i-1}^{n}(x_i - \bar{x})^2} \tag{12}$$

where x_i is the measured value and $\bar{x}$ is the sampled mean of the n number of measurements.

Table 3. T-test coefficients for a two-sided 95% confidence interval.

n	3	5	10	15	20	25	30	∞
$\mathbf{t_{test}(n)}$	4.303	2.776	2.262	2.145	2.093	2.064	2.045	1.960

This probability distribution implies that the actual mean lies within the measured mean plus or minus the error bound calculated from the Student's t-test with 95 % confidence ($\bar{x} \pm Err_{inst}$) (Hines *et al.* 2003).

Conditional errors arise from uncertainties in the measurement conditions including temperature and concentration of NH_3. Based on the stability of the pH measurements described in Section 2.4, the concentration is assumed to be constant for the purpose of this model, and thus, only temperature variations contribute to the conditional errors. Variations in temperature are readily determined as temperature was recorded for

every set of measurements. Absolute uncertainties for the Omega HH-23A digital thermometer using a T-type thermocouple, Omega PHH-103 pH/temperature meter, and Fluke 62 Mini IR thermometer are listed in Table 4.

Table 4. Rated resolution and accuracy of various thermometers used.

Meter	Resolution (°C)	Accuracy (°C)
Omega HH-23A (T-type thermocouple)	0.1	±(0.1 % rdg + 0.6)
Omega PHH-103 pH/Temperature meter	0.1	0.3
Fluke 62 Mini IR thermometer	0.2	±1.5 % rdg or ± 1.5, whichever is greater

The uncertainty in the complex dielectric constant as a result of uncertainties in the measurement of temperature is estimated by calculating the difference between the Meissner and Wentz model for pure water at the measured temperature (T) and the model value at the measured temperature plus the maximum error in temperature measurement (T_{max_dev}) as shown in equation 13.

$$Err_{cond} = Err_{temp} = \left|model(T) - model(T + T_{\max\ \_dev})\right| \quad (13)$$

The total error associated with a sequence of 30 measurements is calculated as the square root of the sum of squares of Err_{inst} and Err_{cond} as shown in equation 14, since the instrumental and conditional errors are uncorrelated.

$$Err_{total} = \sqrt{Err_{inst}{}^2 + Err_{cond}{}^2} \quad (14)$$

315 **3.2 Model Fitting Process**

316 The measured data used for fitting the new model consists of 26 data sets of 30
317 measurement sweeps ranging from temperatures of 1.2 to 23.9 °C and concentrations of
318 0 to 8.5 % NH_3/vol between 2-8.5 GHz as presented in Table 5.
319
320 **Table 5.** Data sets used for model fitting.

Data Set	Date/Time Measured	Concentration (%NH_3/vol)	Temperature (^oC)
1	7/1/2010 - 19:21	0	23.9
2	7/1/2010 - 19:52	0.85	21.7
3	7/1/2010 - 20:13	1.7	21.7
4	7/1/2010 - 20:37	3.4	21.7
5	7/1/2010 - 22:46	8.5	20.0
6	7/1/2010 - 23:39	0	23.0
7	7/2/2010 - 00:07	8.5	20.7
8	7/2/2010 - 00:36	3.4	21.5
9	7/2/2010 - 01:02	1.7	22.1
10	7/2/2010 - 01:28	0.85	22.1
11	7/2/2010 - 01:52	0	22.5
12	1/7/2011 - 01:21	8.5	3.2
13	1/7/2011 - 02:10	3.4	1.9
14	1/7/2011 - 03:02	1.7	1.8
15	1/7/2011 - 03:48	0.85	1.2
16	1/7/2011 - 04:47	0	3.6
7	1/7/2011 - 05:12	0.85	3.0
18	1/7/2011 - 05:41	1.7	3.6
19	1/7/2011 - 13:05	3.4	1.2
20	1/7/2011 - 13:32	8.5	3.2
21	1/7/2011 - 14:39	0	4.2
22	1/7/2011 - 15:11	8.5	4.0
23	1/7/2011 - 15:38	3.4	4.2
24	1/7/2011 - 16:10	1.7	4.8
25	1/7/2011 - 16:35	0.85	5.6

26	1/7/2011 - 17:00	0	6.2

For the model fitting process, an adaptation of the Levenberg-Marquardt optimization algorithm was used (Levenberg 1944, Marquardt 1963). The algorithm used the χ-minimizing function

$$\chi = \sum_{n=1}^{26} \frac{\varepsilon_{measured} - \varepsilon_{model}}{2\sigma_{measured}} \tag{15}$$

where, $\varepsilon_{measured}$ is the measured dielectric constant, ε_{model} is the modeled dielectric constant under model optimization, and $\sigma_{measured}$ is the standard deviation of the measured data. Equation 15 is a modification of minimizing functions used in previous model fitting processes (see, e.g., Hanley et al., 2009, Devaraj et al., 2011). Model fitting for the real component (ε') and imaginary component (ε") of the dielectric constant were conducted independently; however, the model is optimized so as to minimize χ for both components.

The model optimization process fits unknown coefficients of a particular mathematical form so as to minimize the value of χ over all 26 data sets. The Meissner and Wentz (2004) model was used as the basis for the new model. A constraint applied to the new model was that it must match the Meissner and Wentz model when the solution's ammonia concentration equals zero. The model optimization accounts for the temperature, frequency, and concentration dependencies when NH_3 is added to water. The mathematical form for the correction factor that converged across all data sets was

$$\Delta_{NH_3}(C,\nu,T) = \frac{x_{11}\cdot C\cdot \nu^{x_{12}}}{T^{x_{13}}} - j\cdot\left(\frac{x_{14}\cdot C\cdot \nu^{x_{15}}}{T^{x_{16}}} + x_{17}\cdot C\right) \quad (16)$$

where $j=\sqrt{-1}$, C is the volume concentration of NH_3 (between 0 and 0.085 for our experiments), ν is the frequency (in GHz), T is the temperature, and the coefficients x_k are given in Table 6.

Table 6. Coefficients x_k for equation 16.

k	x_k
11	-78.00
12	0.01090
13	0.0586
14	226.4
15	0.0231
16	12.90
17	24.77

When the parameter $\Delta_{NH_3}(C,\nu,T)$ is linearly added to the Meissner and Wentz model for pure water (equation 5), the new model fits the real and imaginary component of the dielectric constants of the laboratory data well, as shown in Figures 6 through 10.

The new correction parameter $\Delta_{NH_3}(C,\nu,T)$ fits 60.26% the experimental data within 2σ uncertainty. Note that $\Delta_{NH_3}(C,\nu,T)$ is non-zero only if the ammonia concentration is non-zero ($C \neq 0$), and thus, the new model is identical to the Meissner and Wentz model when the ammonia concentration is zero.

The resulting new model for the complex dielectric constant of NH_4OH is thus

$$\varepsilon(T) = \frac{\varepsilon_s(T) - \varepsilon_1(T)}{1 + j \cdot \frac{\nu}{\nu_1(T)}} + \frac{\varepsilon_1(T) - \varepsilon_\infty(T)}{1 + j \cdot \frac{\nu}{\nu_2(T)}} + \varepsilon_\infty(T) + \Delta_{NH_3}(C, \nu, T) \quad (17)$$

where $j = \sqrt{-1}$, ν is the frequency in GHz, and $\varepsilon_s(T)$, $\varepsilon_1(T)$, $\varepsilon_\infty(T)$, $\nu_1(T)$, and $\nu_2(T)$ are as defined in equations 6-10. Temperatures are in °C, and equation 16 provides the expression for $\Delta_{NH_3}(C, \nu, T)$.

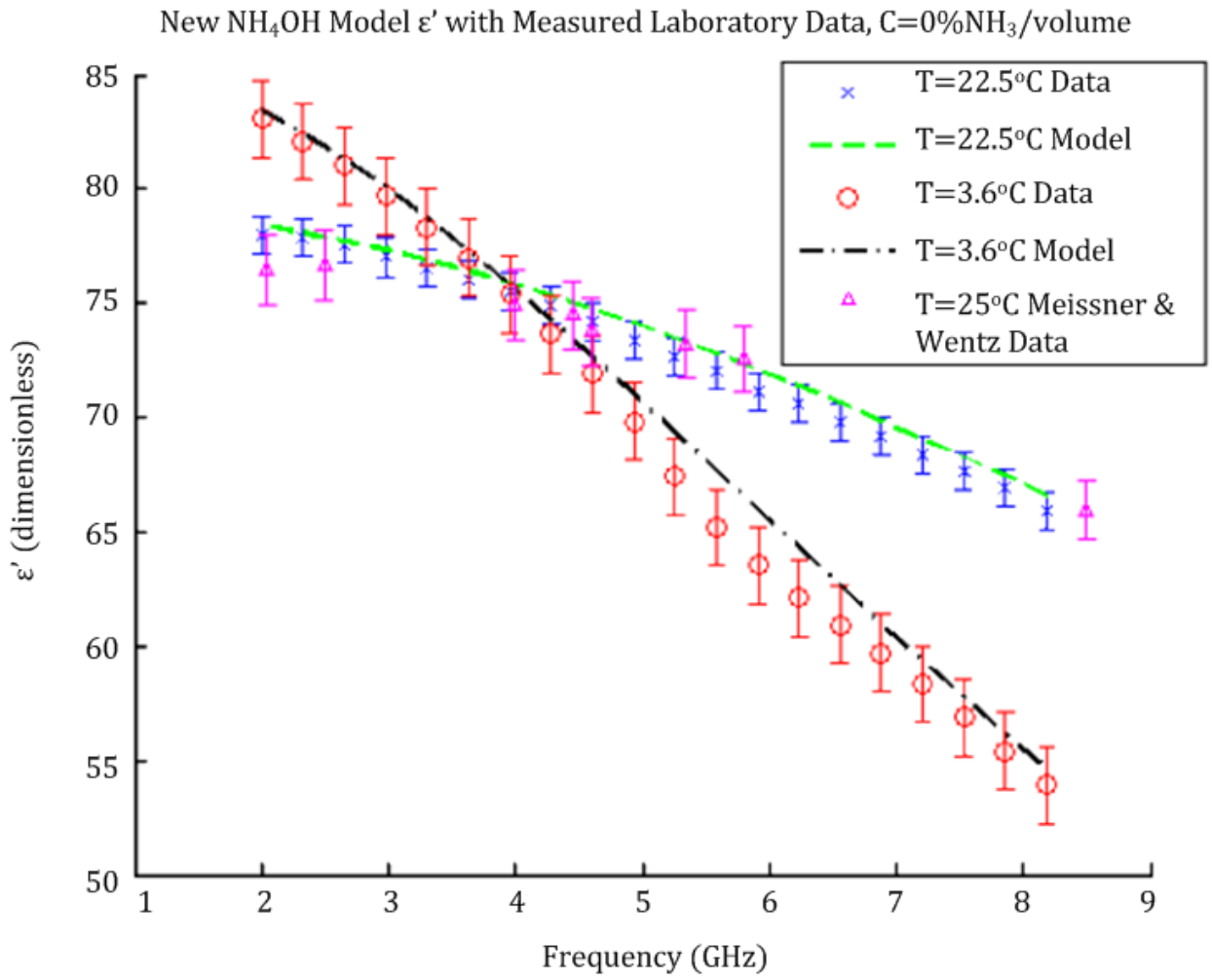

363

364 **Figure 6a.** New model plotted with laboratory data (ε') at zero ammonia concentration and
365 temperatures of 22.5 and 3.6 degrees Celsius. For comparison, datapoints from Meissner and
366 Wentz (2004) taken at 25 degrees Cesius are shown.

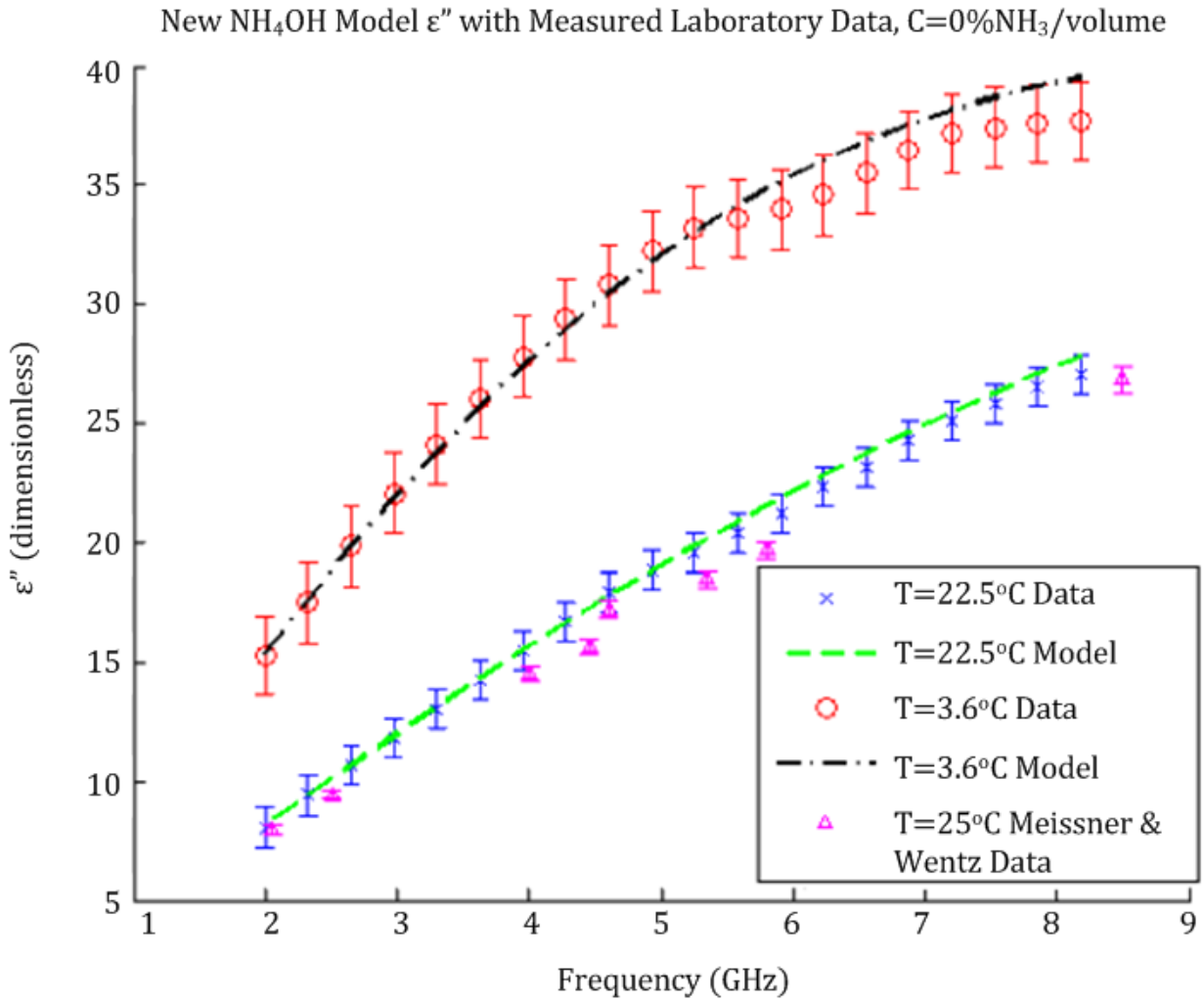

Figure 6b. New model plotted with laboratory data (ε") at zero ammonia concentration and temperatures of 22.5 and 3.6 degrees Celsius. For comparison, datapoints from Meissner and Wentz (2004) taken at 25 degrees Cesius are shown.

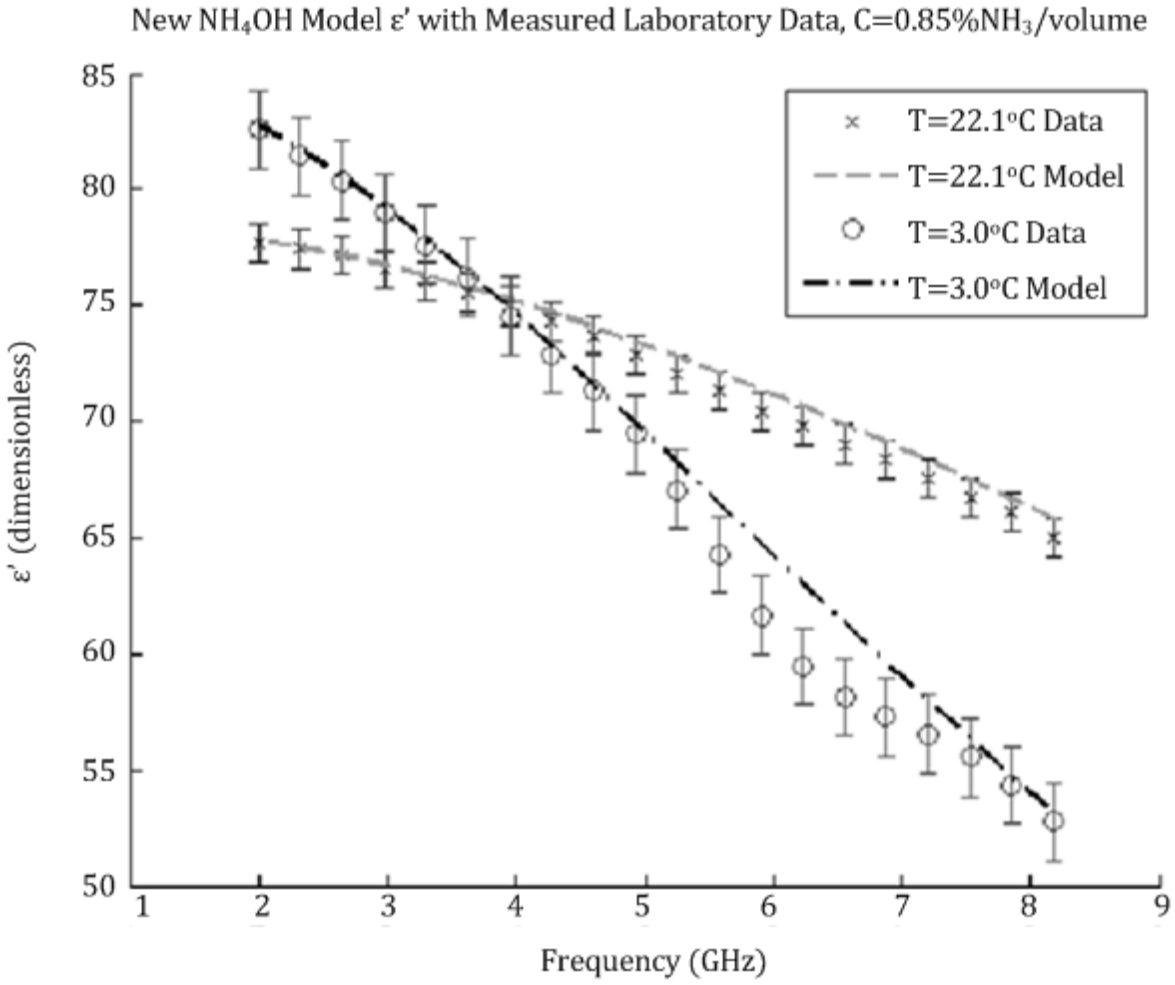

372

373 **Figure 7a.** New model plotted with laboratory data (ε') at 0.85 %NH_3/volume ammonia
374 concentration and temperatures of 22.1 and 3.0 degrees Celsius.
375

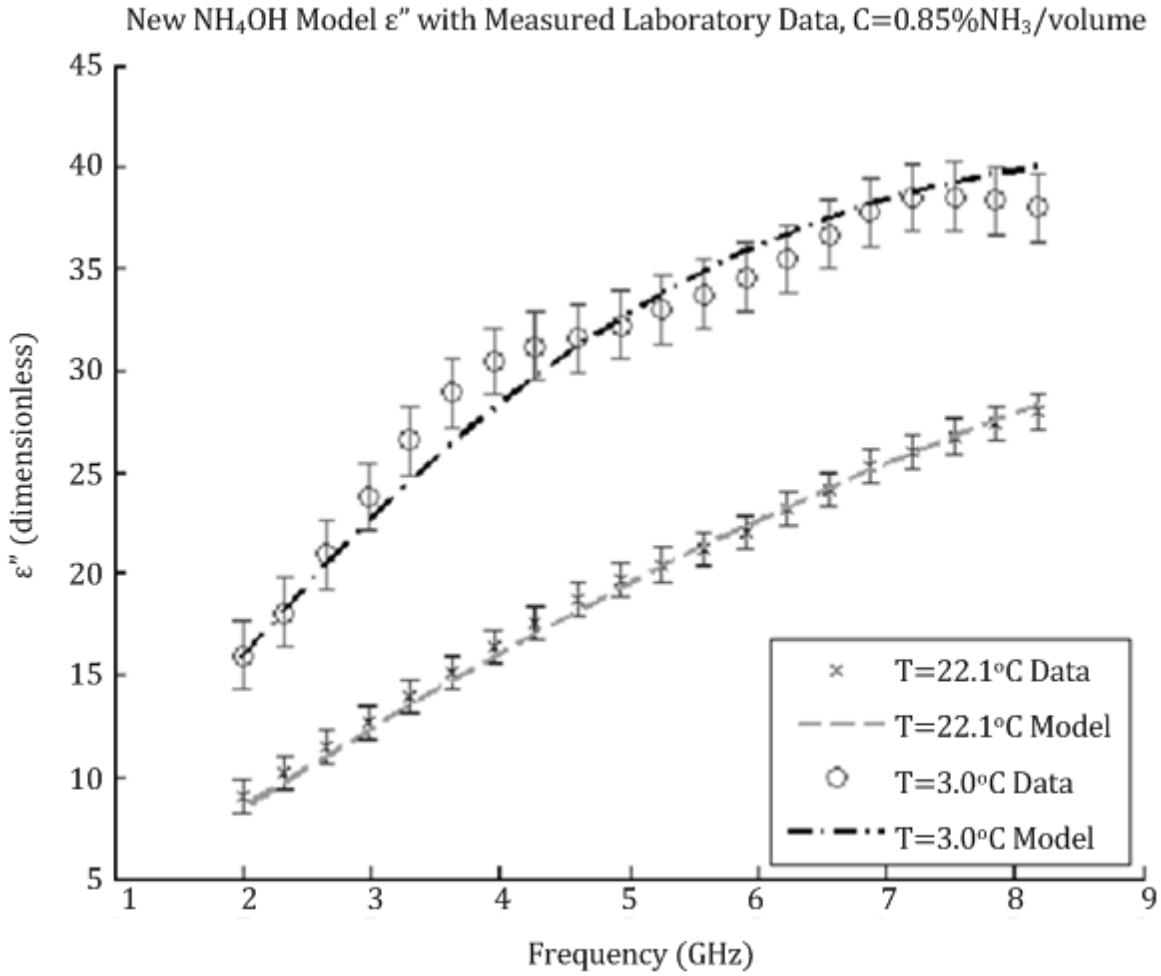

Figure 7b. New model plotted with laboratory data (ε") at 0.85 %NH_3/volume ammonia concentration and temperatures of 22.1 and 3.0 degrees Celsius

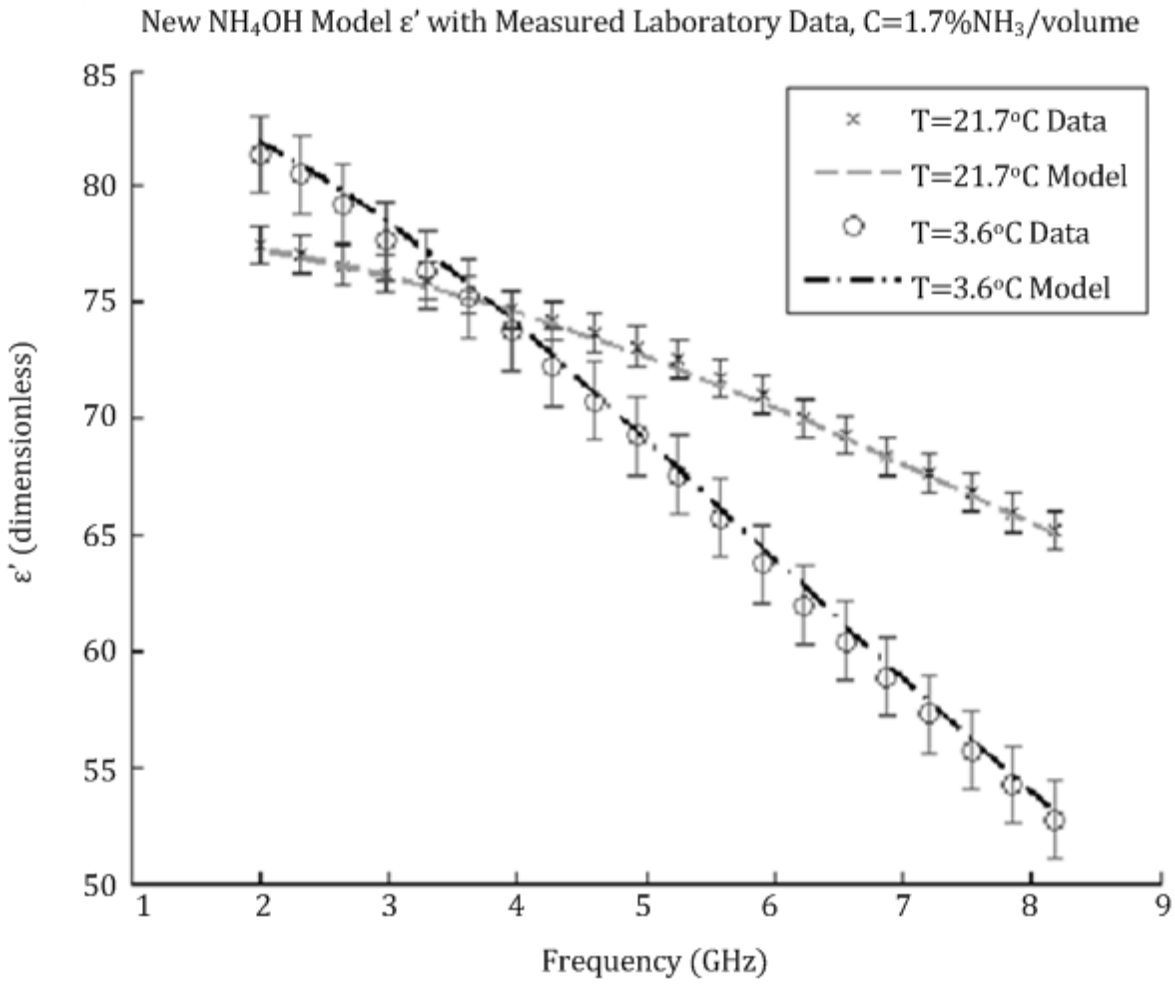

379

380 **Figure 8a.** New model plotted with laboratory data (ε') at 1.7 %NH_3/volume ammonia
381 concentration and temperatures of 21.7 and 3.6 degrees Celsius.

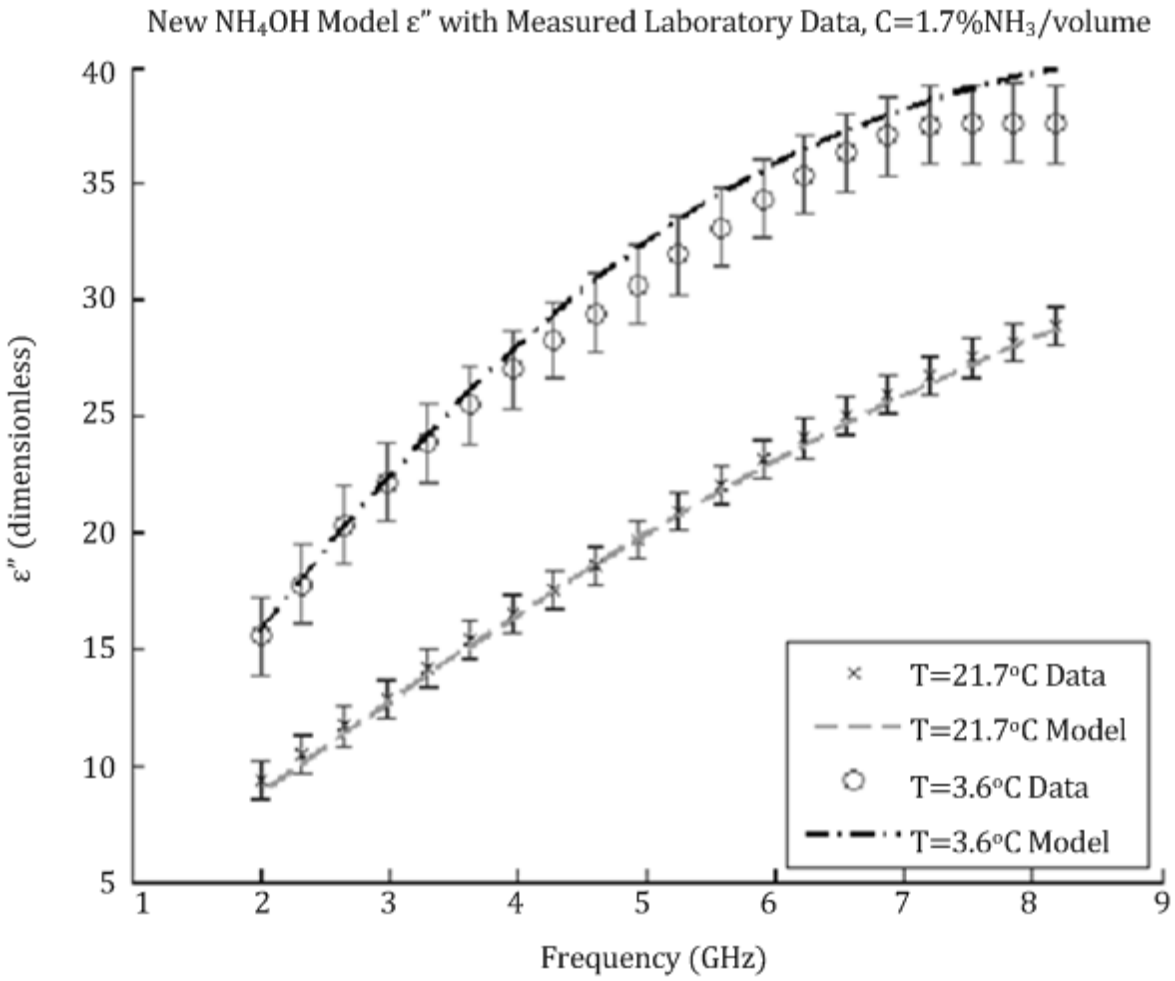

382

383 **Figure 8b.** New model plotted with laboratory data (ε") at 1.7 %NH_3/volume ammonia
384 concentration and temperatures of 21.7 and 3.6 degrees Celsius.

385

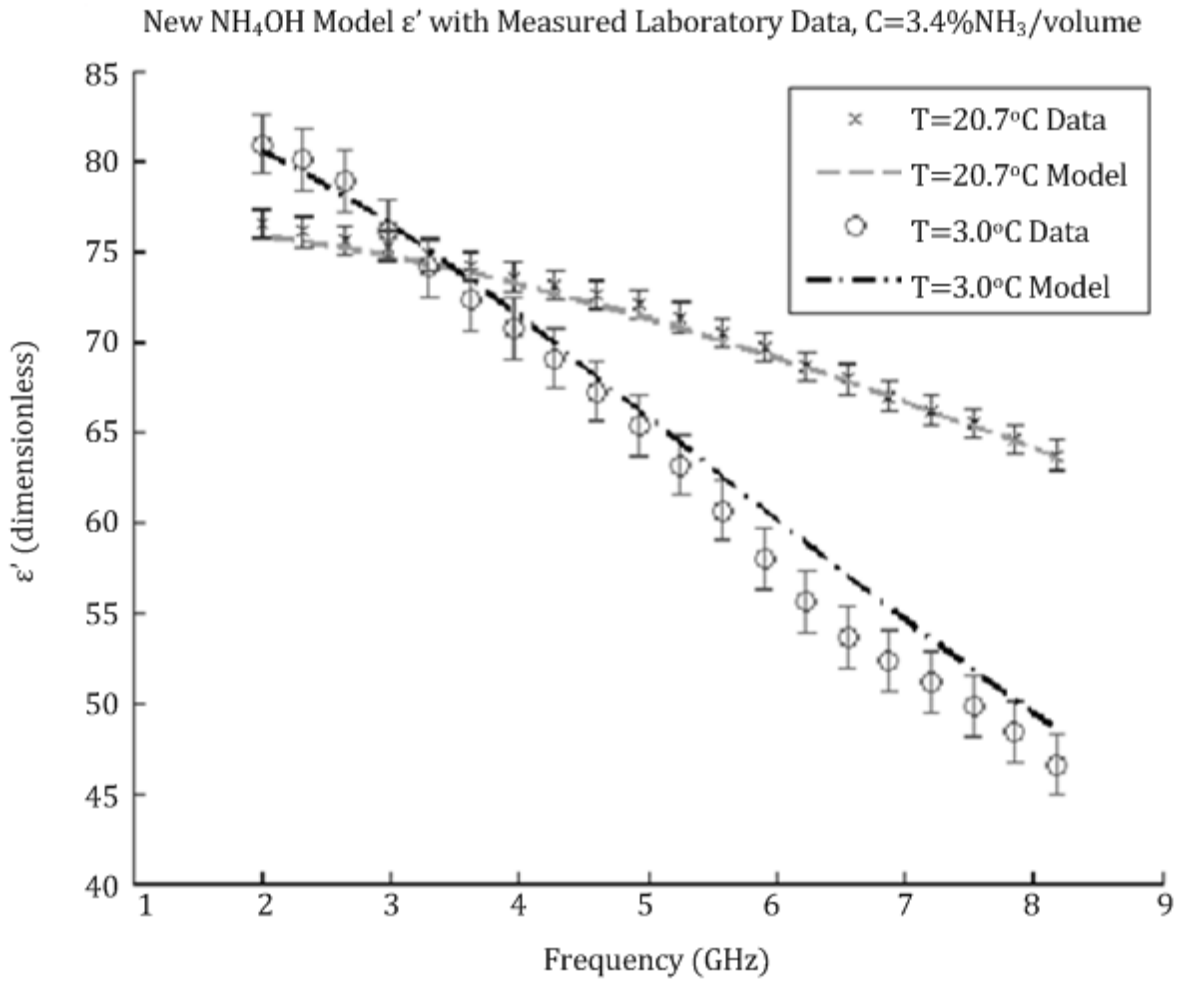

386

387 **Figure 9a.** New model plotted with laboratory data (ε') at 3.4 %NH_3/volume ammonia
388 concentration and temperatures of 20.7 and 3.0 degrees Celsius.

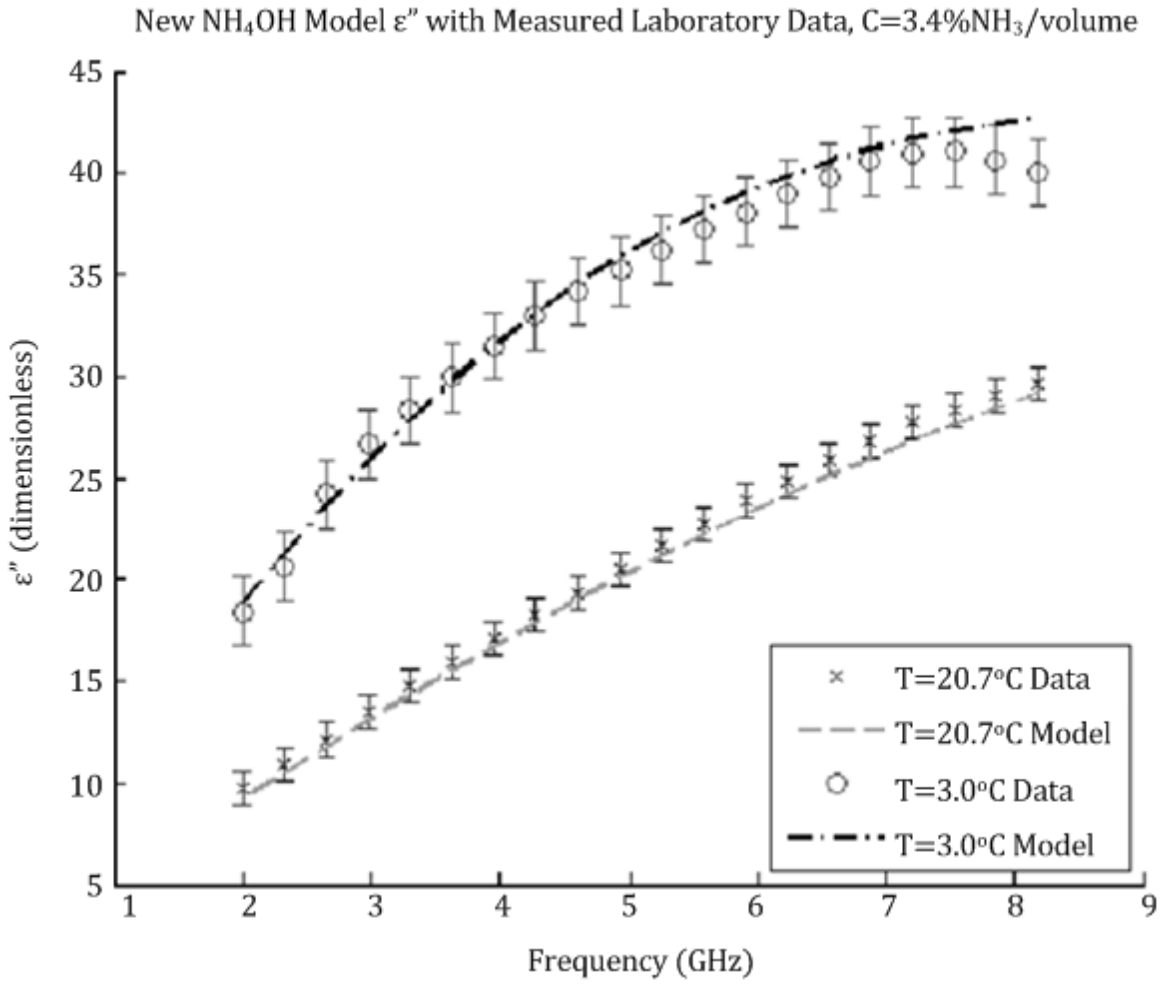

389

390 **Figure 9b.** New model plotted with laboratory data (ε") at 3.4 %NH_3/volume ammonia
391 concentration and temperatures of 20.7 and 3.0 degrees Celsius.

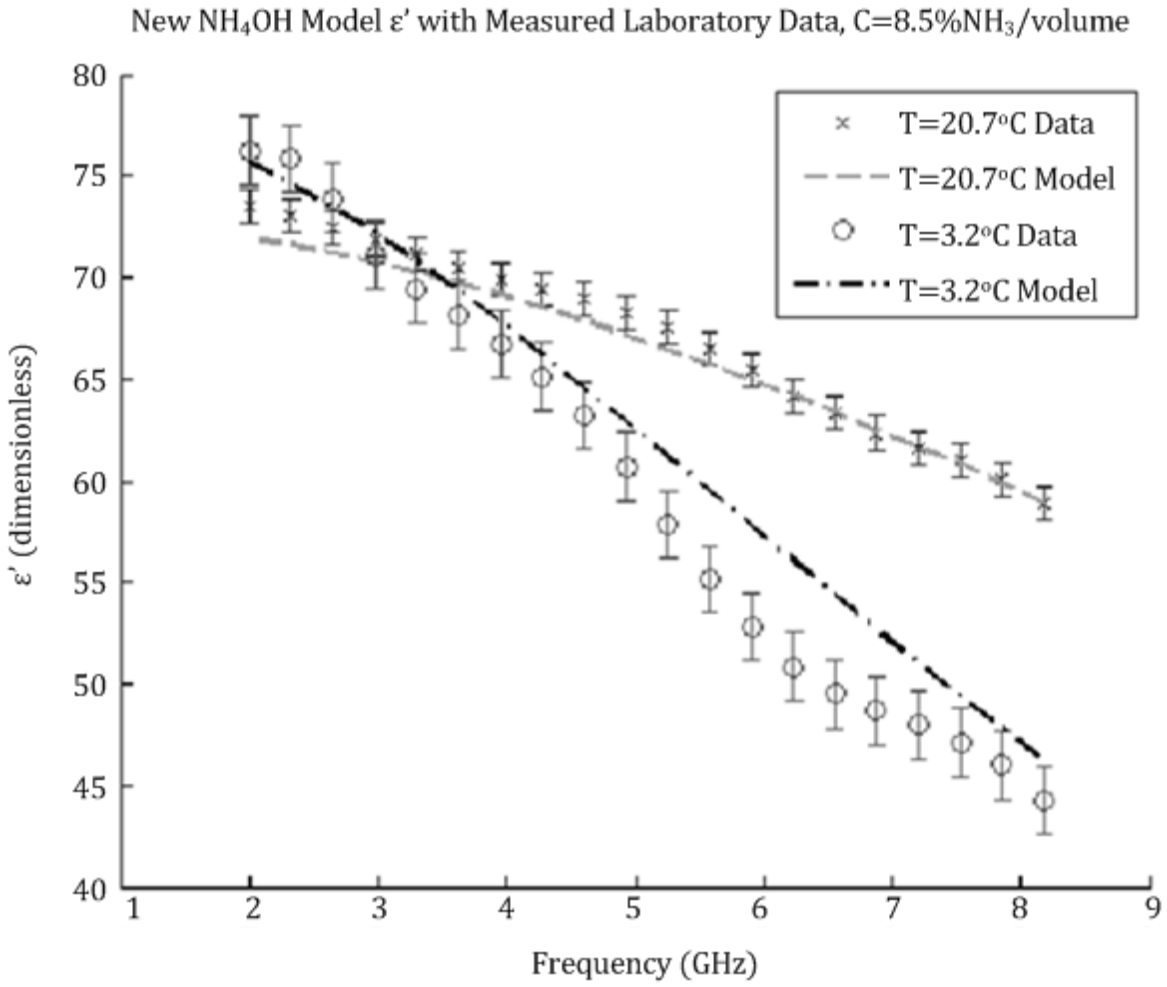

392

393 **Figure 10a.** New model plotted with laboratory data (ε') at 8.5 %NH_3/volume ammonia
394 concentration and temperatures of 20.7 and 3.2 degrees Celsius.

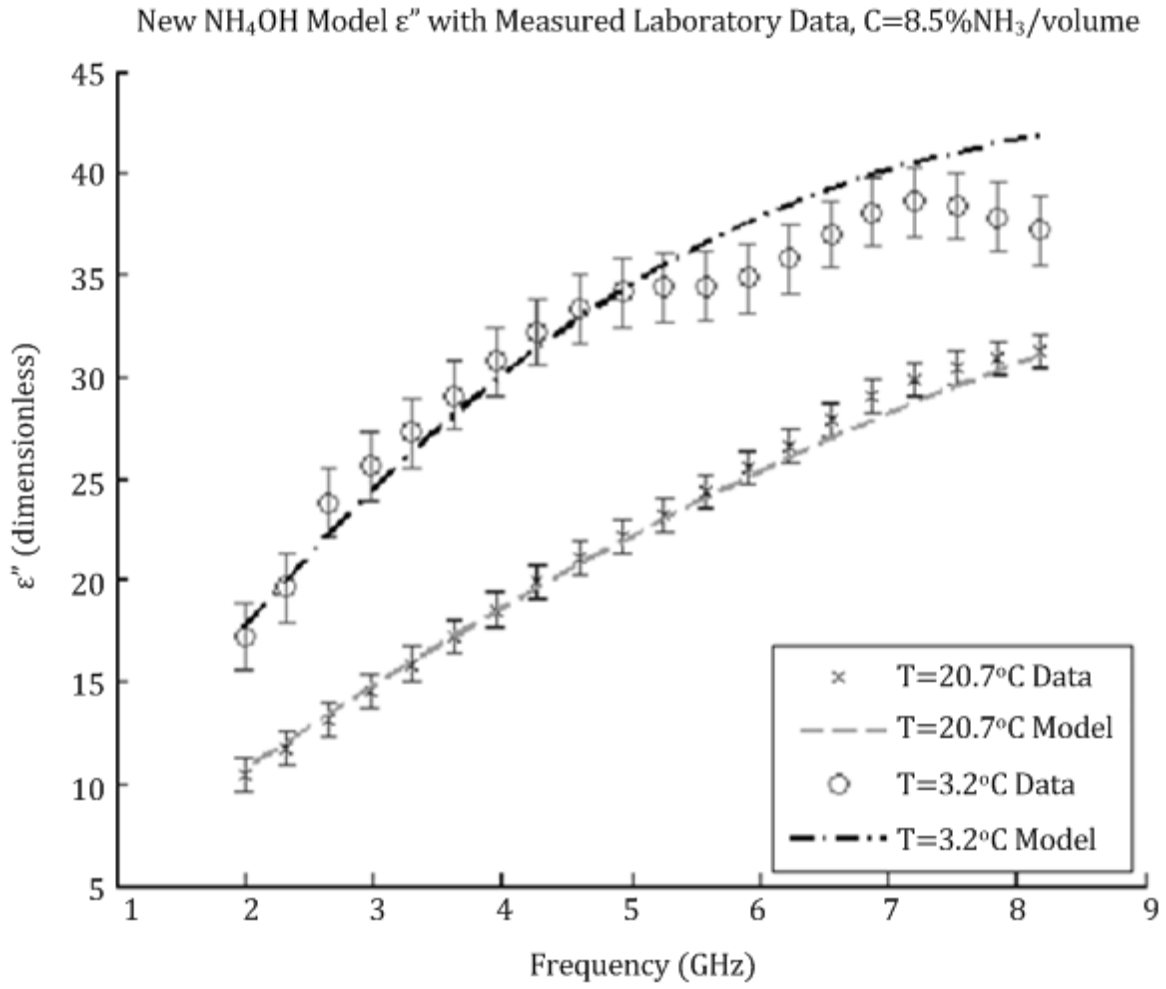

Figure 10b. New model plotted with laboratory data (ε") at 8.5 %NH_3/volume ammonia concentration and temperatures of 20.7 and 3.2 degrees Celsius.

A systematic deviation from the model can be noticed at about 5.5 GHz for the cold temperature measurements. The deviation is likely caused by resonances in the enclosed refrigerator (box resonator) used for these measurements. As the deviations are artificial, the new model's fit of 60.26% of all laboratory data points is likely an underestimation of the true fit.

4. APPLICATIONS

NASA's Juno mission to Jupiter employs a six-channel (0.6, 1.25, 2.6, 5.2, 10, and 22 GHz) microwave radiometer system (MWR, see e.g., Pingree 2008). The spacecraft will enter a highly elliptical polar orbit with a perijove of 1.06 R_J (4,500 km) to pass under Jupiter's synchrotron radiation belts (Matousek 2005). The new aqueous ammonia model is of particular importance for the 2.6 and 5.2 GHz MWR channels. Analyses of the various models for constituent abundances in the deep Jovian atmosphere by Karpowicz and Steffes (2013) show that even under the most generous estimates, aqueous ammonia clouds are only able to form at temperatures at or below ~325 K, which is well within the range of these measurements. Additionally, Karpowicz and Steffes (2013) show that with the same generous estimates, the maximum bulk density, which could be achieved by a Jovian aqueous ammonia cloud would be ~100 g/m^3, which is a range for which Rayleigh scattering would be valid at centimeter-wavelengths.

Assuming Rayleigh scattering, the cloud opacity is obtained from the volume extinction coefficient approximated by (Battan 1973),

$$\alpha_{cloud} = \frac{246 \cdot M \cdot \varepsilon''}{\rho \cdot \lambda \cdot [(\varepsilon' + 2)^2 + (\varepsilon'')^2]} dB/km, \tag{19}$$

where M is the cloud bulk density, ρ is the density of the liquid (water or aqueous ammonia) in the same units, λ is the wavelength in km, and ε' and ε" are the real and imaginary components, respectively, of the dielectric constant of the liquid. The cloud attenuation (extinction) coefficient is expressed in units of dB/km. Note that 1 neper/km = 2 optical depths/km (or km^{-1}) = 8.686 dB/km, where the third notation is used to avoid ambiguities between field extinction coefficients (Nepers/km) and power extinction coefficients (km^{-1}).

The density of the liquid, ρ, varies slightly, depending on the temperature and concentration of ammonia for aqueous ammonia solutions, and estimates of the cloud bulk density, M, are available for the Jovian model (see e.g., Karpowicz and Steffes, 2013). However, assuming the parameters M and ρ to be constant, a percent difference in the cloud attenuation can be calculated using the values of ε' and ε" calculated for water versus those calculated using the new aqueous ammonia model as shown in Figure 11.

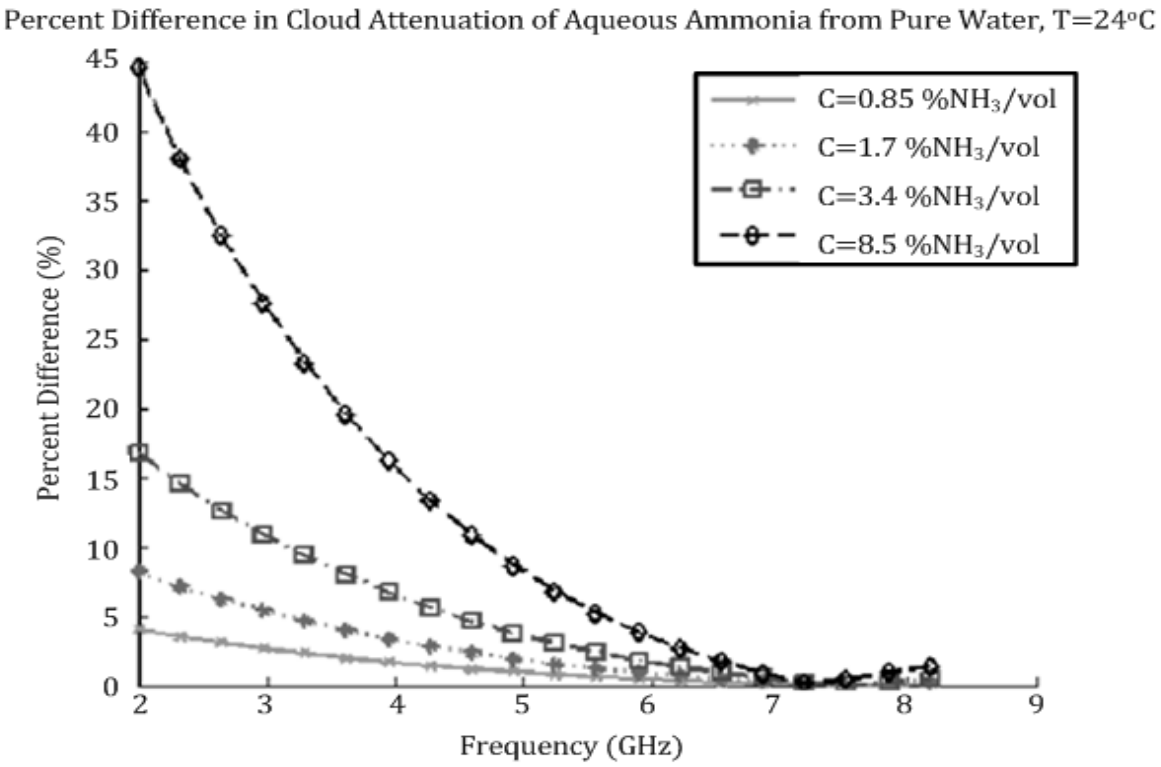

433

434 **Figure 11.** Percent difference in α_{cloud} using the new model versus pure water; assumes
435 parameters M and ρ to be constant in the volume extinction coefficient approximation.

436 As shown in Figure 11, there is a significant difference in the α_{cloud} from aqueous ammonia
437 versus that of water. As this is only a percentage difference, the magnitude of this effect will not
438 be known until the true values for the parameters M and ρ can be applied to the calculation of the
439 volume extinction coefficient in equation 19. However, it is evident that there is a significant
440 increase in α_{cloud} with increasing ammonia concentration. The relative roles of the opacity from
441 various atmospheric constituents on the microwave spectrum of the outer planets has been
442 discussed in several previous works. (See, e.g., Janssen et al., 2005 and 2013).

Current estimates of the dissolved ammonia abundance in the jovian water cloud are between 2-3% (see e.g. Atreya et al., 1999). An example of Jovian aqueous cloud opacity based on a conservative cloud bulk density of 1 g/m^3 and an ammonia concentration of 2.5% NH_3/volume is shown in Figure 12. The temperature is 300 K, and the density, ρ, used in equation 19 is a linear combination of the aqueous ammonia density (ρ_{NH4OH} = 9.853 E 5 g/m^3) and water density (ρ_{H2O} = 9.970 E 5 g/m^3) based on concentration (Weast 1989).

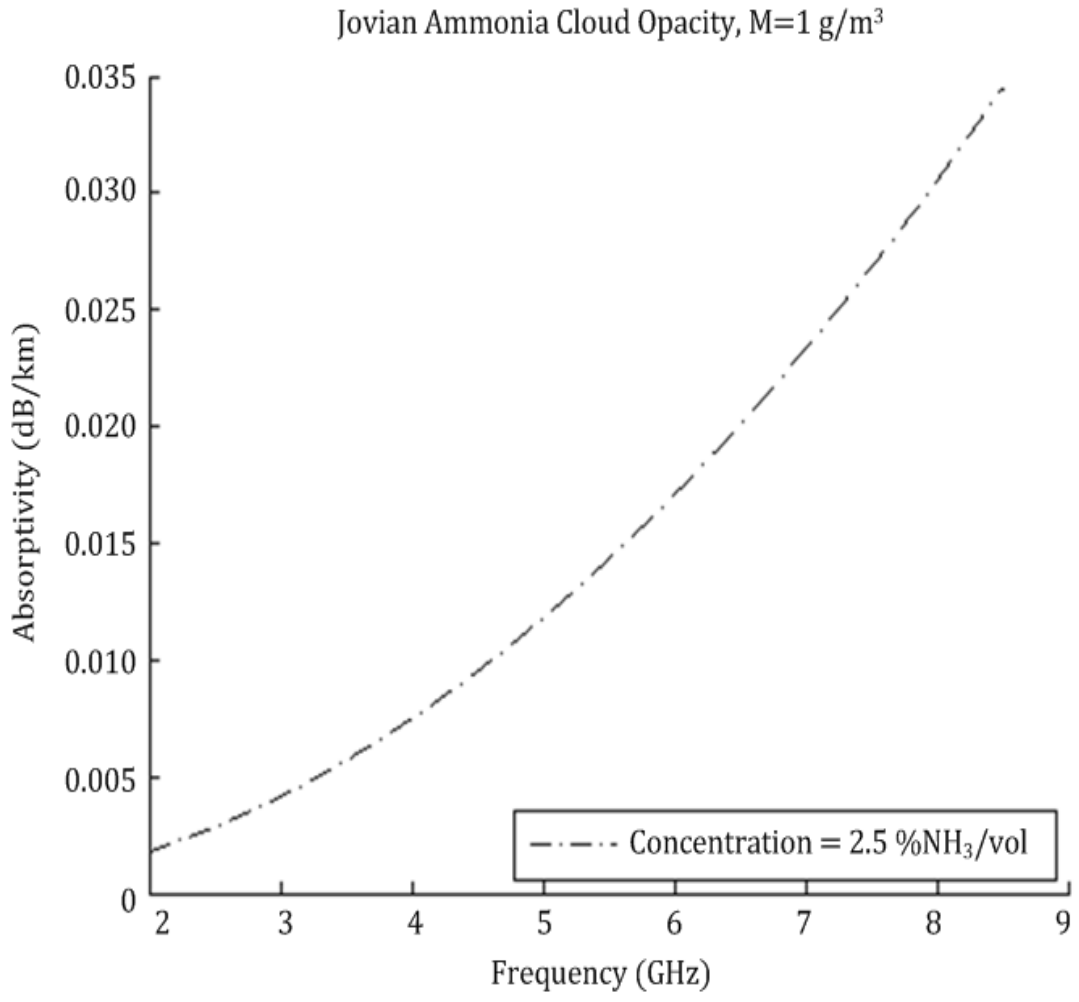

Figure 12. Jovian aqueous ammonia cloud opacity at 300 K with concentration 2.5%NH_3/volume and with a cloud bulk density M=1 g/m^3.

5. CONCLUSIONS

With the recent launch of NASA's Juno probe to Jupiter, knowledge of the complex dielectric properties of aqueous ammonia has become important for characterizing the effect of Jovian clouds on its microwave emission spectrum. No model for the complex dielectric constant of aqueous ammonia had been previously developed, and thus, these results constitute a significant increase in the understanding of the true electromagnetic properties of NH_4OH. The new model for the complex dielectric constant of aqueous ammonia is able to fit 60.26% of the laboratory data within 2σ uncertainty. The ranges verified by laboratory data are from frequencies between 2-8.5 GHz, temperatures from 0-24 °C (273-297 K), and concentrations between 0-8.5 % NH_3/volume. Limited additional measurements at higher temperatures show that the model can be reliably used to temperatures exceeding 40 °C (313 K).

Acknowledgments: This work was supported by NASA Contract NNM06AA75C from the Marshall Space Flight Center supporting the Juno Mission Science Team, under Subcontract 699054X from the Southwest Research Institute.

References

Agilent Technologies 2006. Agilent Basics of Measuring the Dielectric Properties of Materials, 85070E Application Note.

Atreya, S. K., M. H. Wong, T. C. Owen, P. R. Mahaffy, H. B. Niemann, I. dePater, H.B. Niemann, P. Drossart, and T. Encrenaz 1999. A comparison of the atmospheres of Jupiter and Saturn: deep atmospheric composition, cloud structure, vertical mixing, and origin. Planetary and Space Science 47, 1243-1262.

Battan, L. J. 1973. *Radar observation of the atmosphere*, University of Chicago Press, Chicago.

de Pater, I., D. DeBoer, M. Marley, R. Freedman, and R. Young (2005), Retrieval of water in Jupiter's deep atmosphere using microwave spectra of its brightness temperature, *Icarus, Vol. 173*, 425-447.

Devaraj, K., P. G. Steffes, and B. M. Karpowicz (2011), Reconciling the centimeter and millimeter-wavelength ammonia absorption spectra under jovian conditions: Extensive millimeter-wavelength measurements and a consistent model. *Icarus, Vol. 212*, 224-235.

Hanley, T. R., P.G. Steffes, and B.M. Karpowicz 2009. A new model of the hydrogen and helium-broadened microwave opacity of ammonia based on extensive laboratory measurements," *Icarus*, vol. 202, pp. 316-335, July 2009.

Hayt, W., and J. Buck (2006), *Engineering Electromagnetics*, 8th edition. McGrawHill, New York.

Hines, W.W., D. C. Montgomery, D. Goldsman, and C. Borror 2003. *Probability and Statistics in Engineering*, 4th edition, John Wiley and Sons, New York

Janssen, M. A., M. D. Hofstadter, S. Gulkis, A. P. Ingersoll, M. Allison, S.J. Bolton, S. M. Levin, and L. W. Kamp 2005, Microwave remote sensing of Jupiter's atmosphere from an orbiting spacecraft, *Icarus, Vol. 173*, 477-453.

Janssen, M.A., A.P. Ingersoll, M.D. Allison, S. Gulkis, A.L. Laraia, K.H. Baines, S.G. Edgington, Y.Z. Anderson, K. Kelleher, F.A. Oyafuso 2013. Saturn's thermal emission at 2.2 cm wavelength as imaged by the Cassini RADAR radiometer, *Icarus*, vol. 226. 522-535.

Karpowicz, B. M. and P.G. Steffes 2013. Investigating the H_2-He-H_2O-CH_4 equation of state in the deep troposphere of Jupiter, *Icarus*, vol. 223. 277-297.

Levenberg, K. (1944), A method for the solution of certain nonlinear problems in least squares. *Quart. Appl. Math*., Vol. 2, 164-168.

Marquardt, D. (1963). An algorithm for least squares estimation of nonlinear parameters. *SIAM J. Appl. Math*., Vol. 11, 431-441.

Matousek, S. (2005). The Juno New Frontiers Mission, *IAC 2005 Conference*, IAC05A3.2A.04, Fukuoka, Japan.

Meissner, T., and F. J. Wentz (2004), The complex dielectric constant of pure and sea water from microwave satellite observations, *IEEE Transactions on Geoscience and Remote Sensing, Vol. 42*, 1836-1849.

P. Pingree, *et al*. 2008. Microwave Radiometers from 0.6 to 22 GHz for Juno, A Polar Orbiter around Jupiter. *Proceedings of IEEE Aerospace Conference*, Big Sky, MT, March 2008.

Weast, R. C., and D. R. Lide (Eds.) (1989), *CRC Handbook of Chemistry and Physics*, CRC Press.

Highlights – Duong, Steffes, and Noorizadeh "The Microwave Properties of the Jovian Clouds: A New Model for the Complex Dielectric Constant of Aqueous Ammonia

1. Previous models for the microwave emission of the outer planets assumed the microwave opacity from putative aqueous clouds with dissolved ammonia was essentially identical to that from pure water.
2. The described laboratory measurements disclose that the effect of the dissolved ammonia is significant, and should be included in radiative transfer models.
3. The Juno Mission Microwave Radiometer Instrument (Juno-MWR) will provide the first unobstructed view of the microwave emissions from the Jovian atmosphere which are effected by such clouds. These laboratory results will make possible accurate interpretation of such measurements.